DISSERTATIONES SCHOLA DOCTORALIS SCIENTIAE CIRCUMIECTALIS,
ALIMENTARIAE, BIOLOGICAE. UNIVERSITATIS HELSINKIENSIS

18/2016

HANNA AARNOS

Photochemical Transformation of Dissolved Organic Matter in Aquatic Environment – from a Boreal Lake and Baltic Sea to Global Coastal Ocean

DEPARTMENT OF ENVIRONMENTAL SCIENCES
FACULTY OF BIOLOGICAL AND ENVIRONMENTAL SCIENCES
DOCTORAL PROGRAMME IN INTERDISCIPLINARY ENVIRONMENTAL SCIENCES
UNIVERSITY OF HELSINKI

Faculty of Biological and Environmental Sciences
Department of Environmental Sciences
Aquatic Sciences
University of Helsinki
Finland

PHOTOCHEMICAL TRANSFORMATION OF DISSOLVED ORGANIC MATTER IN AQUATIC ENVIRONMENT

FROM A BOREAL LAKE AND BALTIC SEA TO GLOBAL COASTAL OCEAN

Hanna Aarnos

ACADEMIC DISSERTATION

To be presented, with the permission of the Faculty of Biological and Environmental Sciences of the University of Helsinki, for public examination in the Auditorium 1041, Biocenter 2, Viikki (Viikinkaari 5, Helsinki) on 2 September 2016, at 12 noon.

Helsinki 2016

Supervisor: Dr. Anssi V. Vähätalo
Department of Biological and Environmental Science, University of Jyväskylä, Finland

Reviewers: Prof. Roger Jones
Department of Biological and Environmental Science, University of Jyväskylä, Finland

Prof. David J. Kieber
Department of Chemistry, State University of New York, College of Environmental Science and Forestry, USA

Opponent: Prof. Stefan Bertilsson
Department of Ecology and Genetics, Limnology and Science for Life Laboratory, Uppsala University, Sweden

Custos: Prof. Jukka Horppila
Department of Environmental Sciences, University of Helsinki, Finland

ISSN 2342-5431 (online)
ISBN 978-951-51-2358-9 (PDF)
http://ethesis.helsinki.fi

ISSN 2342-5423 (paperback)
ISBN 978-951-51-2357-2 (paperback)

Dissertationes Schola Doctoralis Scientiae Circumiectalis, Alimentarie, Biologicae
Hansaprint, Helsinki 2016

ABSTRACT

As dissolved organic matter (DOM) constitutes a vast reservoir of carbon and nutrients in lakes, rivers and ocean, it plays an important role in the global carbon and nutrient cycle. Only a part of DOM molecules are directly biologically utilizable by bacteria, but solar radiation induced photochemical reactions may mineralize DOM to inorganic forms such as dissolved inorganic carbon (DIC) and ammonium (NH_4^+), and degrade non-labile DOM molecules to labile substrates available for bacteria. This dissertation examined the photochemical transformation of DOM in the surface water in different scales of aquatic environments; from a Finnish boreal lake and the Baltic Sea to the coastal areas of ten globally big rivers. This dissertation studied photochemical reactions such as photoproduction of DIC, NH_4^+, and labile substrates supporting bacterial growth, and determined the photoreactivity of DOM, i.e., apparent quantum yields for the photoreactions in each environment. To consider the relevance of photochemistry of DOM an optical model was used to quantify the photoreaction rates taking into account for the determined photoreactivity of DOM and solar radiation incidental to each environment studied.

In the Baltic Sea, the pelagic heterotrophic bacterioplankton was carbon-limited indicating low bioavailability of DOM in the surface water. Irradiations of the waters with natural or simulated solar light resulted in photobleaching of chromophoric dissolved organic matter (CDOM) and phototransformation of DOM to inorganic carbon and nitrogen as well as labile DOM substrates. This dissertation showed that in the Baltic Sea, the annual photoproduction of ammonium corresponded to 9 – 18% of the annual river loading of DON, but the photoproduction of DIC exceeded the annual river loading of photoreactive DOC. Furthermore, the studies along the salinity transects indicated that terrigenous DOC was more photoreactive than marine DOC. In the Baltic Sea, where also photoammonification was measured, marine DON was more reactive than terrigenous DON. The photoproduced labile substrates supported bacterial production and biomass leading to a 3-level trophic transfer of non-labile DOM and a simultaneous stimulation of autotrophic algae and primary production. The annual amount of photostimulated bacterial biomass corresponded to 3 – 5% of total bacterial biomass across the entire Baltic Sea. In the Baltic Sea as well as in the mesohumic lake studied, the photolytic water layer was shallow and limited the phototransformation of DOM to the top 30 cm.

In the global scale, the annual DIC photoproduction from terrigenous CDOM in front of the ten rivers studied (12.5 ± 2.1 Tg C y^{-1}) corresponded to 18 ± 4% of annual flux of terrigenous DOC of the rivers. When extrapolated to a global estimate, 44.5 ± 10.6 Tg of terrigenous DOC was annually mineralized to DIC by solar radiation in coastal waters. Globally, the amount

of photomineralization of terrigenous DOC was larger in coastal ocean than in lakes and reservoirs. However, the areal rates of DIC photoproduction were larger in the lakes and reservoirs than in the coastal waters indicating that phototransformation of terrigenous DOC was likely limited by relatively short residence times in inland waters. To conclude, the phototransformation in coastal waters formed the final sink for riverine terrigenous CDOM and DOC, but was restricted in general, to a few hundred kilometres from river mouths to the ocean with the exception of largest discharging rivers.

LIST OF ORIGINAL PUBLICATIONS

This thesis is based on the following publications referred to in the text by their roman numerals:

I Hoikkala L., Aarnos H. and Lignell R. (2009). Changes in nutrient and carbon availability and temperature as factors controlling bacterial growth in the northern Baltic Sea. *Estuaries and Coasts* 32:720–733.

II Vähätalo A.V., Aarnos H., Hoikkala L. and Lignell R. (2011). Microbial link through the photochemical transformation of terrestrial dissolved organic matter supports hetero- and autotrophic production in coastal waters. *Marine Ecology Progress Series* 423:1-14.

III Aarnos H., Ylöstalo P. and Vähätalo A.V. (2012). Seasonal phototransformation of dissolved organic matter to ammonium, dissolved inorganic carbon, and labile substrates supporting bacterial biomass across the Baltic Sea. *Journal of Geophysical Research – Biogeosciences*, vol. 117, G01004, doi:10.1029/2010JG001633.

IV Aarnos H., Gélinas Y., Kasurinen V. and Vähätalo A.V. Photochemical mineralization of biologically non-labile riverine DOC to dissolved inorganic carbon in coastal waters (submitted for publication in *Global Biogeochemical Cycles*).

AUTHOR'S CONTRIBUTION TO THE PUBLICATIONS

I R. Lignell planned the study. H. Aarnos implemented the study with L. Hoikkala under the guidance of R. Lignell. L. Hoikkala and R. Lignell analysed the data (including orthogonal regression analysis). L. Hoikkala, H. Aarnos and R. Lignell prepared the manuscript. The article was included in the doctoral thesis of L. Hoikkala.

II A.V. Vähätalo and R. Lignell planned the study. H. Aarnos and L. Hoikkala conducted the laboratory experiments with the guidance and contributions by A.V. Vähätalo (carbon stable isotopes) and R. Lignell (primary production). H. Aarnos was responsible for microscoping. A.V. Vähätalo prepared the manuscript with contributions by other authors.

III H. Aarnos planned the study with A.V. Vähätalo and P. Ylöstalo. H. Aarnos conducted the experimental work with contribution by P. Ylöstalo. H. Aarnos analyzed the data and prepared the manuscript with other authors.

IV H. Aarnos planned the study together with A.V. Vähätalo. H. Aarnos and A.V. Vähätalo organized the global river water sample collection. Y. Gélinas provided samples from St. Lawrence River Estuary. H. Aarnos conducted the experimental work, the data analysis, and the manuscript preparation with contributions by other authors.

CONTENTS

SYMBOLS AND ABBREVIATIONS

$a_{CDOM,\lambda}$	Spectral absorption coefficient of CDOM
CDOM	Chromophoric dissolved organic matter
CO	Carbon monoxide
CO_2	Carbon dioxide
CO_3^{2-}	Carbonate ion
CTDF	Conductivity (salinity), temperature, depth and *in situ* fluorescence
ϕ_λ	Apparent quantum yield spectrum, i.e., photochemical reactivity
$\delta^{13}C$	Carbon stable isotopic signature
DIC	Dissolved inorganic carbon
DOC	Dissolved organic carbon
DOM	Dissolved organic matter
DON	Dissolved organic nitrogen
DOP	Dissolved organic phosphorus
E_a	Activation energy of a chemical reaction
GF/F	Glass fibre filter
HCO_3^-	Bicarbonate ion
H_2CO_3	Carbonic acid
HMW	High molecular weight (> 1000 Da)
HNF	Heterotrophic nanoflagellate
HTCO	High temperature catalytic oxidation
λ	Wavelength (nm)
LMW	Low molecular weight (< 1000 Da)
NH_4^+	Ammonium
NO_3^-	Nitrate
NO_2^-	Nitrite
O_2	Oxygen molecule
·OH	Hydroxyl radical
P	Phosphorus
PAR	Photosynthetically active radiation (400-700 nm)
PO_4^{3-}	Phosphate
POC	Particulate organic carbon
pr	Photochemical production rate
PSU	Practical salinity unit
ROS	Reactive oxygen species
TDN	Total dissolved nitrogen
TDP	Total dissolved phosphorus
TOC	Total organic carbon
UV-A	Ultraviolet radiation 320-400 nm
UV-B	Ultraviolet radiation 280-320 nm
UV-C	Ultraviolet radiation < 280 nm

1 INTRODUCTION

1.1 WHY TO STUDY DISSOLVED ORGANIC MATTER?

Natural organic matter (NOM) is ubiquitous on the Earth, and it appears mostly (95%; Hedges 1992) in dissolved fraction in aquatic environments (dissolved organic matter, DOM). The aquatic DOM constitutes a large pool of bioreactive carbon and thus, plays a substantial role in the global carbon cycle. For example, the amount of carbon in oceanic DOM (662 x 10^{15} g; Hansell et al. 2009) is comparable to the amount of atmospheric carbon dioxide, CO_2 (~750 x 10^{15} g; Siegenthaler & Sarmiento 1993). It has been estimated that if only 1% of oceanic dissolved organic carbon (DOC) degraded per year, the amount of CO_2 released would exceed the amount of CO_2 annually produced by fossil fuel combustion (Hedges 2002). DOM pool also affects light penetration, photosynthesis, and carbon and nutrient dynamics in aquatic environments. Due to the climate change, the concentrations of aquatic DOM generally show increasing trends with the primary sources originating from land (He et al. 2016).

In general, the sources of DOM in surface waters include indigenous primary production (autochthonous sources) and inputs of terrestrial DOM synthesized by terrestrial plants in the catchment (allochthonous sources). In the water column, DOM is generated by processes such as extracellular exudates of phytoplankton (e.g., Nagata 2000), viral lysis or autolysis of planktonic organisms, direct excretory release by all aquatic organisms, “sloppy” feeding of phytoplankton cells during zooplankton grazing (Lampert 1978), and leaching from fecal pellets of zooplankton and protozoa (Jumars et al. 1989). DOM can be considered as non-living organic material, or detritus.

In aquatic environments, a substantial part of carbon may flow from DOM to heterotrophic microorganisms, such as bacteria, flagellates and ciliates (Fig. 1). In this microbial loop (Azam et al. 1983), DOM forms the basis of heterotrophic bacterial growth which is grazed by heterotrophic nanoflagellates (HNF), which are grazed by protozoa such as ciliates (Fig. 1). Mesozooplankton feeds on both heterotrophic and autotrophic microplankton, thus, the microbial loop forms a connection between DOM and the classical plankton food chain typically based on phytoplankton production. Also some mixotrophic algae may assimilate DOM directly (Wetzel 2001), which complicates the planktonic food webs further. In addition to carbon, the DOM pool provides a large potential source of nutrients for heterotrophic bacteria and also for autotrophs in the water column of lakes, rivers and ocean.

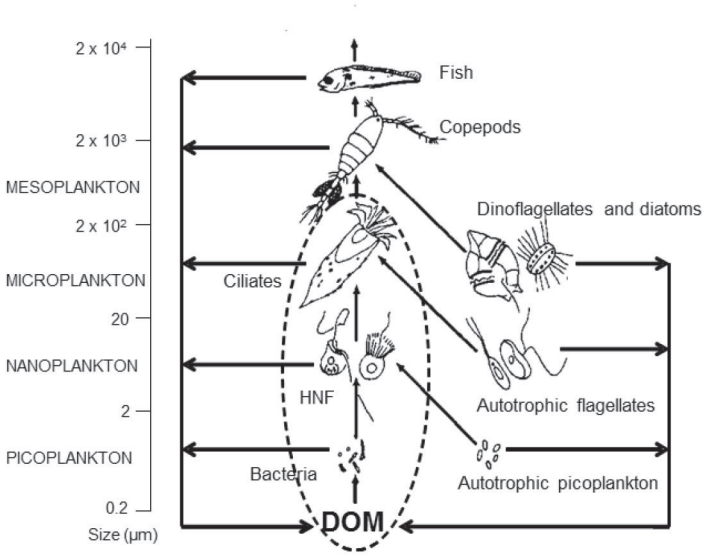

Figure 1 A schematic illustration of microbial loop (circled) and its relationship to the classical plankton food chain. The left and right columns represent heterotrophs and autotrophs, respectively. DOM is released to water column from all trophic levels e.g., via excretion and lysis. Modified from Fenchel 1988.

The dynamics of heterotrophic microorganisms and interaction with DOM (Fig. 1) have important implications for the aquatic carbon cycle. Because the DOM-based food web (left column in Fig. 1) typically contains more trophic levels than the classical food web based on primary production, more carbon is lost by respiration (as CO_2) during the trophic transfer. Further, for example carbon limitation on heterotrophic bacterial growth may indicate that all easily degradable DOC in the water column is consumed and mineralised to CO_2 (Thingstad & Lignell 1997), which is potentially released to atmosphere. When bacterial growth is limited by nutrients, labile DOC is allowed to accumulate in the surface waters and subsequently exported to deep waters, thus, removed from the active carbon cycling. Photochemical decomposition (see below) can be a primary mechanism for removing biologically recalcitrant but photoreactive DOM in lakes (Molot & Dillon 1997) and coastal waters (Nelson & Siegel 2013). In freshwaters, heterotrophic production based on detrital DOM assisted by the photoproduced labile substrates may contribute significantly to the whole ecosystem productivity (Vähätalo 2009). The photochemical mineralization of non-labile DOM and microbial mineralization of labile DOM contribute to the supersaturation of CO_2 in the surface waters and to the export of CO_2 from water to atmosphere. Because of the large pool of reactive carbon in DOM, the biotic and abiotic mineralization of DOM directly influences air-water CO_2 exchange and multiple biogeochemical processes (Medeiros et al. 2015).

1.2 DOM STRUCTURE AND REACTIVITY

Dissolved organic matter consists of a vast reservoir of biochemically heterogeneous organic compounds from simple, low molecular weight (LMW; < 1000 Da) compounds such as amino acids, lipids, and carbohydrates to complex and high molecular weight (HMW; > 1000 Da) compounds such as humic and fulvic acids, cellulose, chitin, and lignin. Dissolved fraction of organic matter is operationally separated from the particulate fraction (particulate organic matter, POM) by filtering with glass fibre filters (GF/F; nominal pore size of ~ 0.7 μm) or membrane filters (0.1 – 0.45 μm). The DOM bioavailability continuum contains e.g., labile DOM molecules that are mineralized on the time scales of minutes to weeks (Amon and Benner, 1996), while DOM molecules resisting microbial degradation may turn over on the time scales of centuries to millennia (Carlson & Hansell 2015). In the ocean, 3% of DOC is considered to be labile for heterotrophic microbes (20 Pg C) compared to 95% of refractory fraction of total DOC (630 Pg C; Hansell 2013). On the other hand, Søndergaard & Middelboe (1995) concluded that 14 – 19% of total DOC is labile in lakes, rivers and seawater.

1.3 DECOMPOSITION OF DOM

Dissolved organic matter can be decomposed in biotic (by microbes) and abiotic processes (by light, pressure or temperature). In natural surface waters, the pressures and temperatures are generally too low to promote decomposition of DOM, and only microbial and photochemical decomposition of DOM takes place.

As presented in the Fig. 1, heterotrophic bacteria can use bioavailable DOM as a carbon and nutrient source. Heterotrophic bacteria alter molecular structure of DOM with enzymatic activities at the cell surfaces, and incorporate labile substrates to bacterial biomass, or mineralize DOC directly to CO_2 by respiration (Carlson & Hansell 2015). Bacteria can directly assimilate only LMW compounds, thus HMW compounds must be hydrolysed to smaller substrates prior the uptake (Amon & Benner 1994). Factors controlling the bioavailability of DOM to heterotrophic bacteria include e.g., the chemical composition of DOM, concentrations of inorganic nutrients, temperature, microbial community structure, and associated enzymes and uptake pathways (Carlson & Hansell 2015). For example in many freshwaters, 50 – 90% of DOM is recalcitrant against microbial decomposition but sensitive to photochemical decomposition (Vähätalo 2009).

1.3.1 PHOTOCHEMICAL DECOMPOSITION

Absorption of solar light is a prerequisite for photochemical transformation of DOM. Colored or chromophoric dissolved organic matter (i.e., CDOM) is a fraction of DOM that interacts with the solar radiation. Especially in many inland and coastal waters, CDOM dominates the absorption of solar radiation (Vähätalo 2009, Nelson & Siegel 2013). CDOM can be considered as a representative of humic substances indicating the terrestrial origin. Thus, less CDOM is found in the open ocean where DOM mainly originates from autochthonous sources (Nelson & Siegel 2013).

The photolytic range of solar radiation spectrum, approximately 290 – 500 nm, is responsible for the phototransformation of DOM in natural waters. The photolytic radiation includes mainly short wavelengths of visible light (400-700 nm) and ultraviolet (UV) radiation. The UV-B (280 – 320 nm) radiation attenuates rapidly into the water column due to the absorption of CDOM and the water molecules, but the role of UV-A (320 – 400 nm) radiation in the DOM phototransformation processes may be larger, as it reaches deeper water columns (Vähätalo 2009). The UV-C (< 280 nm) radiation is absorbed by ozone already in the atmosphere, and thus, does not reach the land (or water) surface. Because the short wavelength radiation is absorbed rapidly in a water column, the photochemical decomposition takes place at the shallow layers of photolytic surface waters.

The photolytic radiation is energetic enough to excite the absorber (e.g., CDOM molecule), even though most of the absorbed energy is released as heat (Mopper et al. 2015). After the excitation, the degradation of photoexcited molecule needs only low activation energy, E_a (e.g., 10 – 30 kJ mol^{-1}), to form radicals and subsequently expulse CO_2, carbon monoxide (CO), or other small molecules (Vähätalo 2009). The excited molecule can also transfer the excitation energy to other molecules, e.g., O_2, which generates reactive oxygen species (ROS; e.g., hydroxyl radicals, ·OH), and thus, consumes O_2 in the water column (Vähätalo 2009). The photoproduced ROS may react with DOM molecules and either increase or decrease the bioavailability of DOM, or directly inhibit the microbial activity (Mopper et al. 2015).

The solar radiation can decompose biologically non-labile DOM (*i*), directly through complete photochemical mineralization or (*ii*), indirectly by increased bioavailability of DOM (e.g., Kieber et al. 1989, Mopper et al. 1991, Lindell et al. 1995, Wetzel et al. 1995, Moran & Zepp 1997, Bertilsson & Tranvik 2000, Miller et al. 2002). The photoproduced LMW carbonyl substrates supporting bacterial growth include e.g., formaldehyde, acetaldehyde, pyruvate, oxalate and other LMW organic acids (Vähätalo 2009, Mopper et al. 2015). Photochemical reactions can stimulate bacterial growth also by releasing inorganic nutrients such as ammonium (Bushaw et al. 1996, Morell & Corredor 2001, Vähätalo & Zepp 2005). However, the

most abundant photoproducts that have been detected in natural waters are CO and CO_2, or more correctly, dissolved inorganic carbon (DIC) i.e., the sum of dissolved CO_2, carbonic acid (H_2CO_3), bicarbonate ion (HCO_3^-), and carbonate ion (CO_3^{2-}; Kieber et al. 1990, Miller & Zepp 1995, Miller & Moran 1997, Bélanger et al. 2006, Mopper et al. 2015). The ratio of CO_2:CO photoproduction ranges from ~2 to >65 (Miller & Zepp 1995, White et al. 2010, Reader & Miller 2012) pointing out that CO_2 is the primary photoproduct in natural waters. The amount of photoproduction of labile organic substrates may equal the photochemical production of CO_2 (Miller & Moran 1997). However, the importance of solar radiation in the decomposition of DOM varies strongly among the aquatic systems (Granéli et al. 1996, Molot & Dillon 1997, Cory et al. 2014).

2 OBJECTIVES

This thesis examined the photochemical transformation of dissolved organic matter (DOM) in different scales of aquatic environments; in a Finnish boreal lake, in the Baltic Sea and in the coastal areas of ten globally big rivers. The main focus of this thesis was in the quantification of photochemical reactions such as photoproduction of dissolved inorganic carbon (DIC; **III**, **IV**), ammonium or labile N (**II**, **III**), and labile DOM supporting bacteria (**I**, **II**, **III**). Special attention is given to the determination of apparent quantum yields for photoreactions, i.e., the photochemical reactivity of DOM. An optical modelling approach was used to study the importance of these photoreactions in each environment.

First, this thesis examined both bacterial and photochemical decomposition of DOM in the northern Baltic Sea during a thermal stratification from spring to late summer (**I**). The nutrient treatment experiments studied the key substrates (inorganic N and P, and labile C) limiting bacterial growth and DOM bioavailability above and below the seasonal thermocline. In the irradiation experiments, the photostimulation of bacterial production and photochemical loss of DOC and DON were determined with vertical distribution along a small-scale salinity gradient.

Secondly, the thesis assessed the response of hetero- and autotrophic plankton to the phototransformation of DOM during a summer N-limitation in the northern Baltic Sea (**II**). The photostimulated production and biomass of heterotrophic bacteria, flagellates and ciliates were examined together with the dynamics of production and community structure of phytoplankton.

Further, this thesis examined direct photochemical mineralization of DOC and DON to DIC and NH_4^+, respectively, and the photoproduction of labile DOM supporting bacterial biomass from the same water samples. The photoreactions were studied along a large-scale salinity gradient in the Baltic Sea during spring, summer, and autumn. These photoreactions were extrapolated to rates over the whole Baltic Sea area according to the salinity dependence of the photoreactions. The importance of phototransformation was assessed by comparing the rates to other C and N fluxes in the Baltic Sea (**III**).

Finally, this thesis studied direct photochemical mineralization of riverine non-labile DOC to DIC in coastal waters in a global scale (**IV**). The photochemical reactivity of riverine terrigenous DOC was studied in a seawater matrix to scale the area of coastal ocean required for the photomineralization of annual riverine DOC flux by each studied river. A global estimate of riverine DOC photomineralization was assessed by using the dependence between the photobleaching of terrigenous CDOM and the photochemical production of DIC in the studied rivers. A salinity gradient (0 – 31) in the St. Lawrence River Estuary was studied more closely.

3 MATERIAL AND METHODS

3.1 WATER SAMPLE COLLECTION

3.1.1 BALTIC SEA

The studies of this thesis were partly conducted in the Baltic Sea (Fig. 2; **I, II, III**). The Baltic Sea is one of the world's largest brackish water basin with a drainage area 4.2 times as large as the sea area (380 000 km^2). This shallow (mean depth of 54 m) and semi-enclosed sea has a water renewal time of 50 yrs (Leppäranta & Myrberg 2009). The large riverine inputs of freshwater (450 km^3 yr^{-1}) and allochthonous material result in a surface water salinity of 0 – 9 (nearly 25 in Kattegat close to the North Sea) and high concentrations of DOC (260 – 480 mmol C m^{-3}) and DON (9 – 23 mmol N m^{-3}; Hoikkala et al. 2015).

Surface water samples were collected to examine the dynamics and reactivity of DOM in coastal waters. For the article **I**, the Baltic Sea samples were collected from three sites along a small-scale salinity gradient (length of ca 35 km): a freshwater end of Pojo Bay (*Pj* in Fig. 2), an outer archipelago site in Långskär (*Lå* in Fig. 2), and an open-sea site at Gulf of Finland with a salinity of ca 6 (*A1* in Fig. 2). Pooled surface (0 – 10 m) waters were sampled by a research vessel in *Lå* and *A1*, but in *Pj* the surface water (2 m) sample was taken from a dock. Additionally pooled deep (20 – 60 m) waters were collected from *A1* for nutrient treatment experiments. The monthly sampling followed a summer phytoplankton succession from the main postspring bloom in May to the late cyanobacterial bloom in August in 2003. As an exception, in July 2003, a pooled surface (0 – 7 m) sample was collected from an inner archipelago site in Storfjärden (*Sf* in Fig. 2) for a nutrient treatment experiment.

For the article **II**, a pooled surface (0 – 5 m) water sample was collected in the outer archipelago site in Långskär (*Lå* in Fig. 2) during a N-deplete period after a spring bloom in mid-May 2005.

For the article **III**, five sampling sites were sampled along a large-scale salinity gradient (length of ca 1200 km): from the salinity of 1 in the Neva Bay (*NB* in Fig. 2) —receiving the largest freshwater discharges of the Baltic Sea by the River Neva— to the salinity of 8 in the Southern Baltic Sea, Arkona Sea (*AS* in Fig. 2). Surface water samples from ca depth of 4 m at the open-sea sampling sites (*AS*, *GB*, *GoF*, and *Hki* in Fig. 2) were collected automatically by a flow-through sampling system in a merchant ship in July and September 2006, and March 2007. Correspondingly, pooled surface (0-3.5 m) water samples were collected by a Limnos-sampler from a research vessel in the Neva Bay (*NB* in Fig. 2).

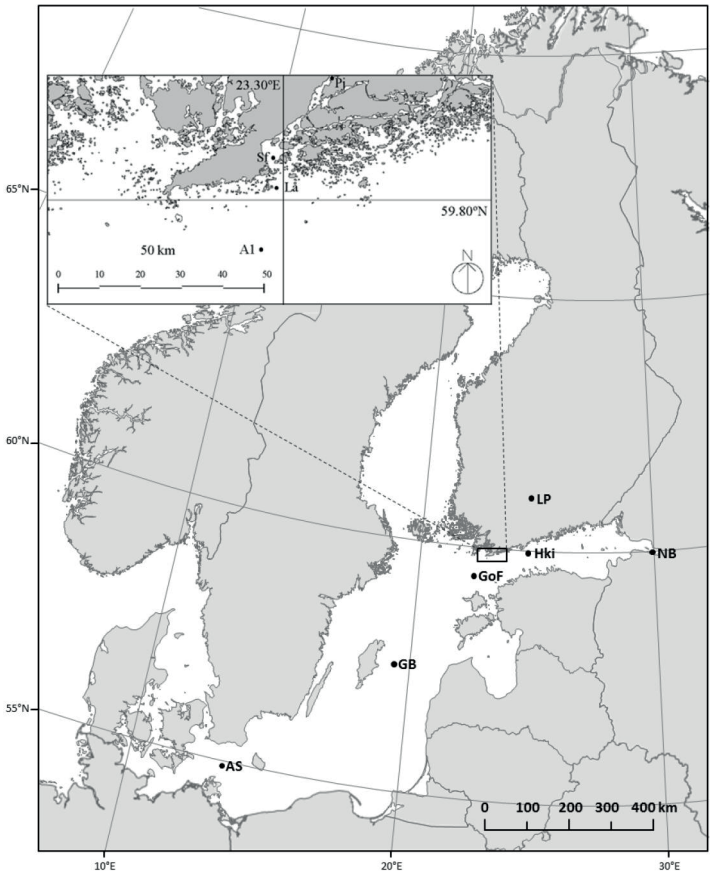

Figure 2 Sampling sites in the Baltic Sea and the Lake Pääjärvi (*LP*; **III**). The large-scale salinity transect (**III**): (*AS*) Arkona Sea; (*GB*) Gotland Basin; (*GoF*) Gulf of Finland; (*Hki*) Helsinki; (*NB*) Neva Bay; and the small-scale salinity transect (**I**): (*A1*) Ajax 1; (*Lå*) Långskär (**II**); (*Sf*) Storfjärden; and (*Pj*) Pojo Bay.

3.1.2 LAKE PÄÄJÄRVI

A freshwater sample from a mesohumic boreal lake in Southern Finland, Lake Pääjärvi (*LP* in Fig. 2) was studied for validation the optical modelling for photomineralization of DOC in **III**. The DOC concentration is about 830 mmol C m^{-3} in Lake Pääjärvi (Arvola et al. 1996). Surface water samples (0 – 1.2 m) were collected by a Limnos-sampler from the middle of the lake in July and August 2007.

3.1.3 BIG RIVERS

The article **IV** of the thesis was conducted with waters collected from globally big rivers: Amazon, Congo, Danube, Ganges-Brahmaputra, Lena, Mekong, Mississippi, Paraná, St. Lawrence, and Yangtze Rivers (Fig. 3). The studied rivers contribute nearly one-third to both freshwater discharge and DOC flux

to the global ocean (Cauwet 2002). They drain 23% of the land area of totally five continents across variable vegetation and climate zones (Milliman & Farnsworth 2011).

For the collection of river water samples (40-L), cleaned and empty polyethylene containers were shipped to the local collaborators at each river. They filled the containers with non-saline water from upstream of the fresh-water – salt-water transition zone during a season of high discharge between March 2009 and June 2010. The samples were thus representative of the DOM discharged to the coastal ocean at the time of sampling. The samples were shipped as such in the dark to our laboratory for experiments on riverine non-labile DOC.

The St. Lawrence River Estuary was examined closer to quantify the direct photomineralization of DOC to DIC. Surface water samples of 1-L (from the depth of 3 m) were collected from seven sites along a salinity gradient (length of ca 450 km) ranging from the freshwater end of the estuary to the salinity of 31 (*A* in Fig. 3) in June 2009. Filtered (0.45 μm) samples were sent in the dark to our laboratory for experiments on natural mixture of riverine and marine non-labile DOC.

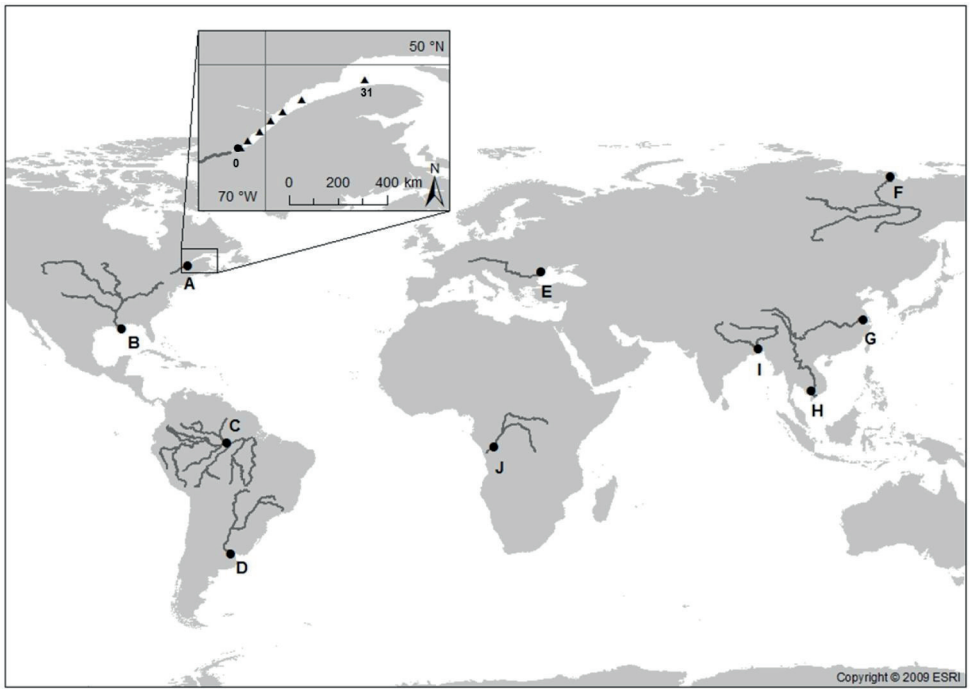

Figure 3 Globally big rivers studied in this thesis: (*A*) St. Lawrence; (*B*) Mississippi; (*C*) Amazon; (*D*) Paraná; (*E*) Danube; (*F*) Lena; (*G*) Yangtze; (*H*) Mekong; (*I*) Ganges-Brahmaputra; and (*J*) Congo. Dots and triangles show sampling locations in the rivers and in the salinity transect (range of 0-31) of St. Lawrence River Estuary, respectively.

3.2 SUMMARY OF METHODS

The methods used in the nutrient treatment and irradiation experiments are presented in the Table 1 and described in detail in articles **I**-**IV**.

In the article **IV**, the photochemical mineralization of riverine non-labile DOC to DIC was examined in a seawater matrix with ten rivers. In this experiment, only concentrations of DOC and photoproduced DIC, and CDOM absorbance were followed (Table 1). However, the same river waters as in **IV** have been studied earlier e.g., for the molecular composition of DOM (Wagner et al. 2015), photochemical isotopic fractionation of DOC (Lalonde et al. 2014), dissolved black carbon (Jaffé et al. 2013), and the contribution of iron to CDOM (Xiao et al. 2013), hence several background parameters have been determined but excluded from this thesis and **IV**.

3.3 NUTRIENT TREATMENT EXPERIMENTS: FACTORS CONTROLLING BACTERIAL GROWTH (I)

In the nutrient treatment experiment (**I**), factors limiting bacterial growth and biological decomposition of DOM were studied with inorganic N and P and glucose-C treatments in the surface (0 – 10 m) and deep water (20 – 60 m) samples from the thermally stratified open-sea site *A1* at the Gulf of Finland, Baltic Sea (Fig. 2). The GF/F-filtered surface and deep water samples were treated with eight (control without treatment, N, P, NP, C, NC, PC, and NPC), or four (control without treatment, C, NP, and NPC) combinations of nutrient additions, respectively. The levels of added nutrients were corresponding to the concentrations found in the deep water in the Gulf of Finland (see details in **I**). The nutrient-treated samples were incubated in the dark for 3 d. As the *in situ* temperature (at the surface water) increased during the study season, the incubation temperatures were 10 °C in May, 16 °C in June, and 18 °C in July and August. The deep water samples were incubated at the same temperatures, except in August (13 °C). Additionally, control and NPC-treated deep water samples were incubated at the *in situ* temperature of 3 °C.

Bacterial production, biomasses of bacteria and heterotrophic nanoflagellates, and concentrations of organic (DOC, DON) and inorganic nutrients (NH_4^+, NO_3^-, PO_4^{3-}) were measured during the incubations (see methods in Table 1).

Table 1 *Summary of the methods used in the nutrient treatment (I) and irradiation experiments (I-IV). The numbers refer to 1 = H. Aarnos, 2 = other author, and 3 = external service, - not used in article, * measured only as background information before experiments.*

	Parameter	Method	I		II	III	IV
			Nutrient	Light	Light	Light	Light
Water chemistry	NH_4^+	Phenolhypochlorite method	3	-	3	1	-
	NO_3^-, NO_2^-	Reduction of NO_3^- to NO_2^-; colorimetric determination of NO_2^-	3	3	3	3	-
	PO_4^{3-}	Colorimetric determination with molybdate method	3	-	3	3	-
	TDP, DOP	Colorimetric determination after persulphate oxidation; DOP = TDP - PO_4^{3-}	3	-	3	3	-
	DOC, TDN, DON	High temperature catalytic oxidation (HTCO); DON = TDN – (NH_4^+ + NO_3^- + NO_2^-)	1, 2	1, 2	1, 2	3	1
	Total carbohydrates	Ferricyanide oxidation of free reducing sugars, spectrophotometric detection	1, 2	-	-	-	-
	POC, PON, POP	Filtration on GF/F filters and determination with mass spectrometer (POC); or with HTCO (PON/P)	-	-	3	-	-
	$\delta^{13}C$	Filtration on GF/F filters and determination with mass spectrometer	-	-	2	-	-
	CDOM	Spectrophotometric detection	-	1, 2	1, 2	1	1
	Chlorophyll-*a*	Spectrophotometric detection	2*	-	2	-	-
	DIC	'Bubbling chamber' method by Salonen 1981	-	-	-	1, 2	1
Bacteria	Biomass	Epifluorescence microscopy of acridine orange stained cells; cell volumes with Image analysis	1	1	1	1	-
	Bacterial production	^{3}H-thymidine method	1, 2	1, 2	1, 2	-	-
Phytoplankton and protists	HNF biomass	Epifluorescence microscopy of proflavine stained cells; cell volumes with New Porton grid	1	1	1	1	-
	Biomass of small-sized (< 2 µm) autotrophs	Phase contrast microscopy of proflavine stained cells	3*	-	1	-	-
	Biomass of large-sized (> 2 µm) autotrophs and ciliates	Phase contrast microscopy of Lugol´s solution stained cells	3*	-	1	-	-
	Primary production	^{14}C method	-	-	2	-	-
Environmental parameters	Temperature, salinity	CTDF sensor	3*	1, 2*	2*	1, 3*	-
	In situ radiation	Photosensors/ spectroradiometer	-	3*	2	1, 2	-

3.4 IRRADIATION EXPERIMENTS

3.4.1 IN SITU –EXPERIMENT IN THE BALTIC SEA (I)

The photochemical decomposition of DOM and its effects on bacterial growth were studied in surface waters collected from three sites along a small-scale salinity gradient in the Gulf of Finland (**I**; Fig. 2). The experiment was repeated in May (with a water sample from *A1*; Fig. 2), June (*Pj*, *Lå*, and *A1*), July (*Lå* and *A1*), and August (*Pj*, *Lå*, and *A1*). Freshly collected, particle-free filtered waters sealed in 220-mL quartz glass bottles were exposed to natural sunlight in the sea at depths of 10, 30, 70, and 200 cm nearby the site *Sj* (Fig. 2) for 6 – 8 h. Corresponding dark control samples were kept in the dark next to the irradiated samples in the sea. After the light exposure, the irradiated samples and the dark controls were incubated with ambient bacteria (< 0.8 μm) and nutrients (NP and control without nutrient treatment) in the dark for 5 d. The incubation temperatures and levels of nutrient additions followed the ones used in the nutrient treatment experiments for surface water samples (**I**).

DOC and DON concentrations and CDOM absorption were measured before and after the light exposure as well as during the 5-d-long bacterial incubation (see methods in Table 1). Additionally, bacterial production, biomasses of bacteria and heterotrophic nanoflagellates, and concentrations of inorganic nutrients (NH_4^+, NO_3^-, PO_4^{3-}) were followed during the bacterial incubations (details in **I**).

3.4.2 IN SITU –EXPERIMENT IN THE LAKE PÄÄJÄRVI (III)

For validation of the optical model used in **II**-**IV** (Eq. 2 in this thesis), the measured and modelled rates of direct photomineralization of DOC to DIC were assessed for the surface water of Lake Pääjärvi (Fig. 2).

The DIC photoproduction *in situ* in the lake was measured by exposing particle- and DIC-free water samples (details in **III**) sealed in 12-mL quartz tubes to natural sunlight at depths of 2 – 20 cm for 24 h. The dark control samples were kept in the dark next to the irradiated samples in the lake. The concentrations of photoproduced DIC and CDOM absorption in irradiated and dark control samples were determined as described in Table 1. The solar radiation was measured with a spectroradiometer next to the lake over the time of the light exposures in July and August 2007 and corrected by the albedo of lake to quantify the radiation incident to the lake (details in **III**).

The DOC photomineralization rate over the water column (*pr*; mol C m^{-2} d^{-1}) was calculated by integrating the measured rates over the depths (Eq. 1):

$$(1) \qquad pr = \int_{z_{min}}^{z_{max}} pm_0 e^{(-K_{d,pm}\, z)}\, dz$$

where pm_0 is the rate at a depth of 0 m (mol C m^{-3} d^{-1}); $K_{d,pm}$ is the extinction coefficient for photomineralization (m^{-1}); z is the depth (m); and the integration goes through a depth of 0 m (z_{min}) to an infinite depth (z_{max}).

For the comparison of measured and modelled rates, the same lake water sample was irradiated also with a solar simulator in a laboratory for 19 h to quantify the modelled DIC photoproduction as described in Ch. 3.4.3.2. The modelled and measured (*in situ*) rates were then compared after taken the differences in the irradiation temperatures (5 °C and 17 – 19 °C, respectively) into account (details in **III**).

3.4.3 STUDIES ON NON-LABILE DOM (II-IV)

The photransformations modelled in the articles **II**-**IV** focused in biologically non-labile DOM. Thus, the bioavailable DOM was removed in pre-treatments by ambient microbiota prior to the photochemical experiments. The conditions during the pre-treatments and irradiations are summarized in Table 2 (see details in **II**-**IV**).

For irradiation exposures, particle-free water samples were divided into quartz tubes (**IV**) or quartz bottles (**II**, **III**) and into corresponding dark control samples wrapped with aluminum foil. In **III** and **IV**, the exposures were carried out with a solar simulator (Atlas Suntest CPS+) with a maximum intensity of 765 W m^{-2}. In **II**, natural sunlight was used for the exposure and its intensity was measured with a global radiation sensor. The warming of the irradiated and dark control samples were avoided by keeping the samples in a temperature controlled water bath during the irradiations.

Table 2 *Pre-treatment and irradiation conditions (details in **II-IV**). NL = non-labile; BB = bacterial biomass; - not used in article.*

		II	III	IV
	Focus of the study	NL-DON	NL-DOM	NL-DOC
	Study site	Baltic Sea	Baltic Sea, Lake Pääjärvi	Ten big rivers, St. Lawrence Estuary
Pre-treatment	Sample filtrate	0.2-µm + 10-µm	GF/F	1-µm
	Duration	6 d	4-37 d	40 d – months
	Temperature (°C)	10	22-24	5
	Dark vs light	Light:dark cycle under PAR	Dark	Dark
	Nutrient addition	PO_4^{3-}	-	-
Irradiation	Source of radiation	Sun	Suntest	Suntest
	Sample volume (mL)	220	170	12
	Duration	12 d	46-71 h	39-43 h
	Temperature (°C)	12-15	5	21
	Parameters followed	See Table 1	DIC, NH_4^+, BB	DIC

3.4.3.1 Photomineralization of DON to ammonium (III)

The direct photomineralization of DON to NH_4^+, i.e., photoammonification, was determined by irradiating the particle-free waters as described above

and in Table 2. After the irradiation, the CDOM absorption and the concentrations of NH_4^+ were measured from the initial, dark, and irradiated samples (Table 1; details in **III**). The difference between the irradiated and the dark control samples indicated the amount of photoammonification.

3.4.3.2 Photomineralization of DOC to DIC (III, IV)

The direct photochemical mineralization of DOC was defined as a photoproduction of DIC. In **IV**, non-labile terrigenous DOC was irradiated in a seawater matrix to mimic the coastal conditions by mixing the river samples (1:1) with artificial seawater but the samples from the St. Lawrence River Estuary were examined as such. Before exposing the particle-free mixtures and the estuary samples (**IV**) or the sea and the lake water samples (**III**) to simulated sunlight, the background DIC was removed by acidifying and bubbling the samples with CO_2-free air. The pH was adjusted back to the initial pH prior to the irradiations (Table 2; details in **III**, **IV**).

The concentrations of photoproduced DIC and absorption by CDOM were measured from the initial, dark control and irradiated samples after the irradiation (see methods in Table 1; details in **III**, **IV**). The photochemical mineralization of DOC was calculated as the difference in the DIC concentrations between irradiated and dark control samples.

3.4.3.3 Photoproduction of labile substrates supporting hetero- and autotrophs (II, III)

To study the heterotrophic bacterial response to photoproduced labile carbon substrates (**III**), the particle-free water samples were first irradiated in a similar manner as the photoammonification samples and under the conditions shown in Table 2. Then, the irradiated and the corresponding dark control samples were incubated with indigenous bacteria (GF/F filtrate) and N and P nutrients in the dark at 22 – 24 °C for 7 – 12 d. The growth of bacterial biomass was followed daily (see methods in Table 1). The magnitude of photostimulus in the bacterial biomass turned to bacterial carbon was calculated from the difference between the irradiated and the dark control samples at the highest bacterial cell densities of the incubation (details in **III**).

The article **II** examined the responses of both hetero- and autotrophic plankton to photoproduction of bioavailable DOM and N. The pre-treated and particle-free filtered sample water was exposed to natural sunlight in an outdoor pool as described above and in the Table 2 (details in **II**). After the solar exposure, an indigenous plankton community (10-µm filtrate) was added to the irradiated and the dark control samples, and the waters were incubated at 10°C under PAR for 12 d. Several chemical and biological parameters (Table 1) were determined during the 12-d-bioassay.

3.5 OPTICAL MODELLING OF PHOTOREACTION RATES

The modelling approach used in the articles **II-IV** is applied from the paper Vähätalo et al. (2000). The modelled photoproduction rate, pr_{mod}, for a photoproduct (e.g., DIC, NH_4^+, or labile substrates supporting bacteria) is a product of three spectra (Eq. 2):

$$(2) \qquad pr_{mod} = \int_{\lambda_{min}}^{\lambda_{max}} \phi_\lambda \, Q_\lambda \left(a_{CDOM,\lambda} \, a_{tot,\lambda}{}^{-1}\right) d\lambda$$

where ϕ_λ is the determined apparent quantum yield spectrum for a photoreaction (Eq. 3; mol of photoproduct mol photons^{-1}). Q_λ represents the spectrum of mean annual photon flux density *in situ* (mol photons m^{-2} yr^{-1} nm^{-1}) estimated for each season in the Baltic Sea (details in **II**, **III**) or in the coastal ocean in the front of each studied river (details in **IV**). The ratio $a_{CDOM,\lambda}$ $a_{tot,\lambda}{}^{-1}$ (dimensionless) is a contribution of CDOM to the total absorption coefficient $a_{tot,\lambda}$ (m^{-1} nm^{-1}) equalling to 1, if CDOM absorbs all photons. The integration through λ_{min} to λ_{max} accounts for the wavelengths contributing to a photoreaction.

The apparent quantum yield spectrum, ϕ_λ, describes the amount of photoproduct (mol of DIC (**III**, **IV**), NH_4^+ (**III**), or labile C (**II**, **III**) or labile N (**II**) bound in bacterial biomass) produced per amount of photons absorbed in the sample. The ϕ_λ was assumed to increase exponentially with decreasing wavelength (Eq. 3):

$$(3) \qquad \phi_\lambda = ce^{-d\lambda}$$

where c (dimensionless) and d (nm^{-1}) are positive constants, and λ is the wavelength (nm). The parameters c and d of Eq. 3 were iterated through an unconstrained nonlinear optimization ('fminsearch' function of Matlab; see details in **II**-**IV** and Supplementary materials therein).

3.6 CONTAMINATION PRECAUTIONS

To avoid contamination, all glassware and plastic bottles and containers used in **I**-**IV** were rinsed with detergent and tap water, 6 – 15% hydrochloric acid, and finally with ion-exchanged water. Additionally, all quartz- and glassware and glass fibre filters (GF/F) were precombusted at 400 – 450 °C for at least 2 h. The containers, sample bottles and filters were rinsed thoroughly with sample water prior to use.

4 RESULTS AND DISCUSSION

4.1 FACTORS CONTROLLING BACTERIAL GROWTH

Bacterial growth and DOM bioavailability were investigated in four nutrient treatment experiments throughout a summer when the natural surface and deep water bacterial samples from the open-sea site, Gulf of Finland, were incubated with different inorganic N and P and glucose-C combinations and at different incubation temperatures for 3 d (**I**). In the surface samples, the principal factor controlling bacterial production was bioavailable C. The glucose-C addition increased bacterial production through the study period from May to August, but led rapidly to inorganic nutrient limitation. After the postspring bloom in May and during the summer nutrient minimum in June and July (details in **I**), the combined glucose-C and inorganic N addition significantly increased the bacterial production. During the cyanobacterial bloom in August, also inorganic P was needed in the addition to N and C for a significant response in the bacterial production. A significant response in the bacterial biomass was produced only with the combination of glucose-C and both inorganic nutrients throughout the summer. Overall, the results support the earlier findings that the bacterial growth is limited by both bioavailable carbon and nutrients in the northern Baltic Sea (Lignell et al. 1992, Kuparinen & Heinänen 1993, Lignell et al. 2008). The grazing did not control the bacterial growth in **I**, as no quantifiable numbers of heterotrophic nanoflagellates were found in the GF/F-filtrates after 3-d incubations.

In the deep water samples, the absence of bioavailable C combined with the low water temperature (< 10 °C) limited the bacterial growth. Further, no inorganic nutrient addition affected significantly the bacterial production (details in **I**) because the inorganic nutrient concentrations remained high in the deep waters throughout the summer.

As the bacterial growth was C-limited, the bioavailability of DOM was evidently low in the Gulf of Finland (**I**). Despite of the high share of total carbohydrates (34 – 43% of total DOC) both in the deep and the surface waters, the bioavailability of DOC remained generally small, indicating that the prevailing carbohydrate pool was mainly biologically refractory in the Gulf of Finland. As seen in the concentrations of DOC and DON (**I**), the low bioavailability led in an accumulation of DOM in the surface water during the summer.

4.2 PHOTOTRANSFORMATION OF DOM

Exposing water samples to solar radiation – either natural or simulated – resulted in the phototransformation of DOM in all irradiation experiments. As the absorption of solar radiation in DOM molecules is a prerequisite for occurrence of any photoreactions, the decrease in absorption coefficient spectra of chromophoric DOM ($a_{CDOM,\lambda}$) was noticed in all irradiation experiments, thus, solar radiation photobleached CDOM (**I**-**IV**). For example in **IV**, the irradiations photobleached on average 45% of terrigenous CDOM at 300 nm among the studied rivers.

The photochemical reactions transformed DOM to labile forms, which clearly increased the biomass (**II**, **III**) and the production (**I**, **II**) of heterotrophic bacteria, as well as stimulated the growth of heterotrophic flagellates and ciliates (**II**). Bacteria grew faster, the cell densities were higher and the cell volumes bigger in the irradiated samples than in the dark control samples resulting in a photostimulus of 77 – 765% in the bacterial biomass e.g., in **III**. Also e.g., Moran & Zepp (1997) have noticed a similar 1.5- to 6-time increase of bacterial production and biomass due to the photoproduction of labile DOM substrates.

In the *in situ* -experiment in the Baltic Sea (**I**), the concentrations of DOC and DON were generally not significantly different between the irradiated and the dark control samples after the 6 – 8-h long irradiations in the sea. Obviously, the small amount of photodecomposition of DOC and DON was not detectable against the high background concentrations of DOC and DON. The irradiation neither had consistent effects on the bacterial biomass. However, the irradiation induced a small but consistent decrease (on average 3.7%) in $a_{CDOM,375}$ (**I**). Also the bacterial production integrated over time increased significantly in the irradiated samples after incubating the samples with ambient bacteria for 5 d (Fig. 4 in **I**) indicating the photoproduction of labile substrates from photoreactive CDOM. The pronounced response in bacterial production was seen only with the samples irradiated at the depth of 10 cm (see details in **I**). The samples irradiated at the deeper depths (30, 70, and 200 cm) did not differ from the dark control samples suggesting that the layer of photolytic reactions facilitating bacterial growth is < 30 cm in the light exposure site *Sj* in the Gulf of Finland.

The article **II** demonstrated a 3-level trophic transfer of biologically non-labile DOM in a "microbial loop" as photoproduced labile DOM stimulated the heterotrophic bacteria, which was then grazed by heterotrophic nanoflagellates, which were eventually grazed by ciliates. This shows that the trophic transfer of photoproduced DOM is not limited only to humic waters (De Lange et al. 2003, Daniel et al. 2006), but also takes place in coastal waters. Additionally, **II** showed an increase in phytoplankton biomass and production in the irradiated water samples compared to the dark controls. The exposure of biologically non-labile DOM to natural solar radiation supported both heterotrophs and autotrophic algae, with differing responses

among phytoplankton taxa (details in **II**). As the plankton community was N-limited during the 12-d bioassay, phytoplankton was likely stimulated by the photoproduction of labile N, primarily as NH_4^+ but in smaller amounts also as amino acids (Tarr et al. 2001, Vähätalo 2009). Also mixotrophy, i.e. phytoplankton using bacteria as a source of N, which is a common strategy for algae to obtain nutrients under oligotrophic conditions (Zubkov & Tarran 2008), may have explained the stimulation of certain phytoplankton taxa (see details in **II**).

The dynamics of the plankton induced by the phototransformation of DOM agreed with the dynamics of particulate organic carbon (POC) and nitrogen (PON) during the 12-d bioassay (**II**). The bacterial biomass, POC and PON increased at the expense of photoproduced DOM, which led to the trophic transfer and the stimulation of primary production followed by the respiratory losses of POC at the end of bioassay (see Fig. 1 in **II**). In the terms of C:N stoichiometry, the photoproduced DOM first lowered the C:N ratios of plankton, indicating that bacterioplankton preferentially incorporated photoproduced N than C. Later the biological processes, such as grazing, modified the C:N ratios of plankton similar to the ones of the dark control samples (see Fig. 1 in **II**). The carbon stable isotope signature ($\delta^{13}C$) indicated that POC and the biomass of plankton were primarily based on the phototransformed allochthonous DOM imported from the catchment of the Baltic Sea (details in **II**).

Also the differences in DIC (**III**, **IV**) and NH_4^+ (**III**) concentrations between the irradiated and the dark control samples were significantly higher than those between the dark and the initial waters, indicating that photochemistry was responsible for the mineralization of DOC and DON directly to DIC and NH_4^+, respectively. In **IV**, the DIC photoproduction was linearly dependent on the photobleaching of terrigenous CDOM with a regression coefficient of 0.00402 mol C m^{-2} (R^2 = 0.96; Fig. 1 in **IV**).

4.3 APPARENT QUANTUM YIELDS

The amount of photoproduced DIC (**III**, **IV**), NH_4^+ (**III**), and labile DOM supporting bacteria (**II**, **III**) was normalized with the amount of absorbed photons for the determination of apparent quantum yield spectrum, ϕ_λ (Eq. 3). Fig. 4 represents the ϕ_λ spectra for the photoreactions studied in this thesis with the comparable ϕ_λ spectra from the literature. The parameters for calculating the ϕ_λs (Eq. 3) are reported in the articles **II**-**IV**. This thesis and many previous studies describe ϕ_λ with two parameters resulting in spectra which increase exponentially towards shorter wavelengths (Fig. 4 and references therein). However, some studies use three parameters for ϕ_λ resulting in a slightly different shape of ϕ_λ (Bélanger et al. 2006; Reader & Miller 2012; Fig. 4B).

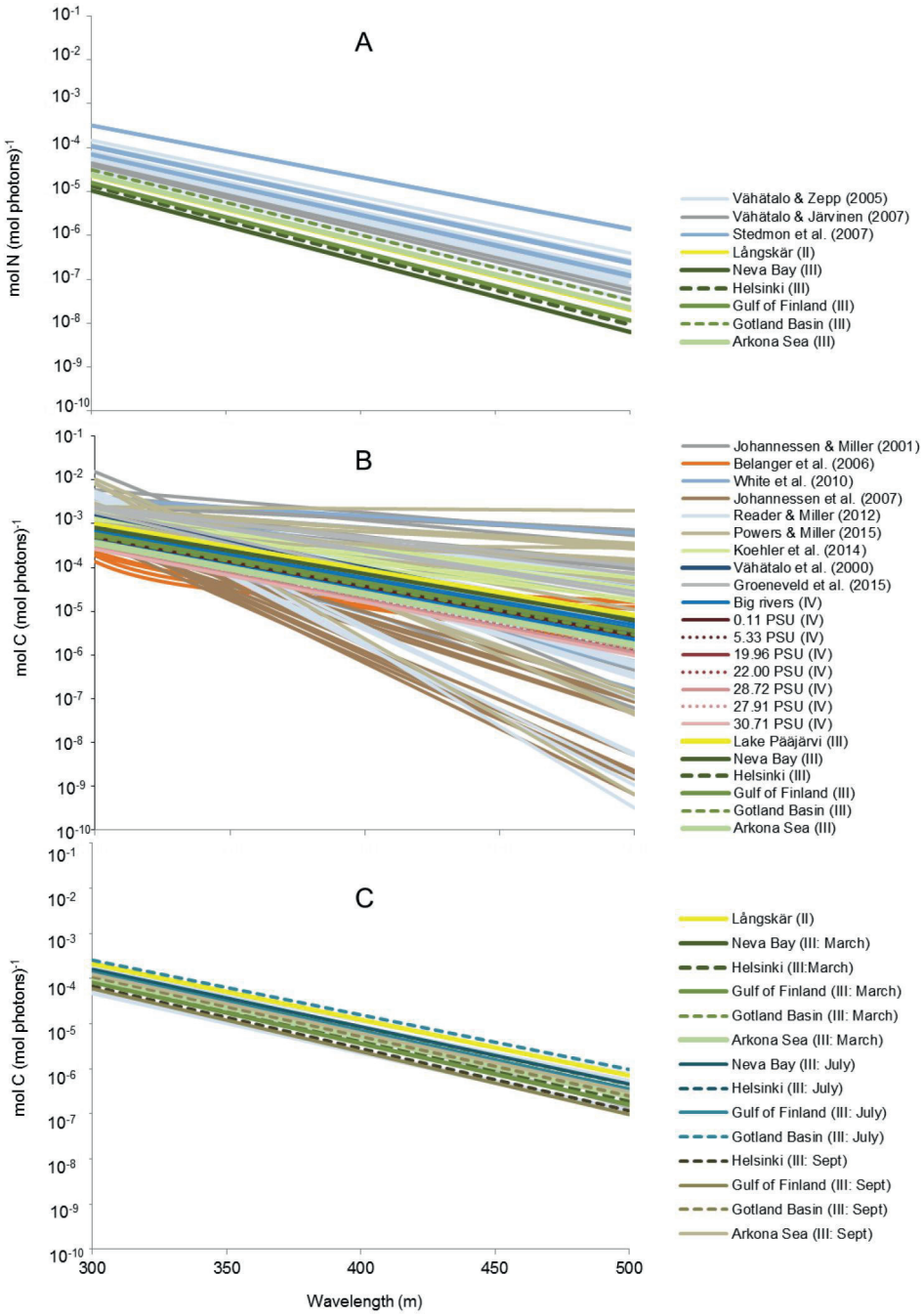

Figure 4 Apparent quantum yield spectra for the photoreactions studied in **II-IV** and from the literature. The photoreactions presented in the panels: (A) photoproduction of NH_4^+ and labile N; (B) photomineralization of DOC to DIC; and (C) photoproduction of labile DOM supporting bacterial biomass. Note the logarithmic scale on y-axis.

The ϕ_λs determined in **II-IV** generally fit in the range of earlier published values (Fig. 4). The long irradiation times and thus, high doses of photons used for determination of ϕ_λs in this thesis may have led to lower ϕ_λs due to the photobleaching of photoreactive CDOM during irradiations (Andrews et al. 2000; Vähätalo & Wetzel 2004). Especially the spectra for photoammonification ($\phi_{NH4,\lambda}$; **III**) was lower than previously determined in the Baltic Sea (Fig. 4A; Vähätalo & Zepp 2005; Stedmon et al. 2007; Vähätalo & Järvinen 2007). The low temperature (+5 °C) used in **III** prevented the microbial interference during the irradiation, but obviously slowed the photoammonification rate. Thus, when calculating the photoreaction rates with the ϕ_λs (Eq. 2) in **III**, the temperature correction was taken into account (details in **III**).

The ϕ_{DIC} spectra for the studied ten rivers are represented more distinctly in Fig. 2 in **IV** but they are also drawn in Fig 3B here. The photoreactivity of terrigenous DOC ($\phi_{DIC,330}$) was highest in the Mississippi River and nearly three-fold compared to the lowest $\phi_{DIC,330}$ in the Ganges-Brahmaputra River, indicating a high variability in the photoreactivity of terrigenous DOC between the studied rivers running through different climate and vegetation areas.

The ϕ_λs for photoproduction of labile DOM supporting bacterial biomass determined in **II** and **III** are the first published estimates (Fig. 4C). With these estimates, it is possible to calculate directly the photoproduction of labile DOM supporting biomass and its contribution to the heterotrophic production and to higher trophic levels.

4.4 SEASONALITY

In the articles **I** and **III**, the phototransformation of DOM (and the factors limiting bacterial growth) in the Baltic Sea were followed over a summer phytoplankton succession or over three seasons (spring, summer, and autumn), respectively.

Seasonality had no impact on the concentrations of DOC or DON in the Baltic Sea (**I**, **III**). Neither the ϕ_λs determined for photoproduction of DIC and NH_4^+ showed significant difference between the seasons (**III**), thus the data from the seasonal irradiation experiments were pooled to iterate a mean ϕ_λ for each photoreaction and site (Fig. 4A and B). The lack of seasonality in $\phi_{DIC,\lambda}$ and $\phi_{NH4,\lambda}$ was unexpected, because the photobleaching of CDOM potentially decreases the photochemical reactivity of DOM during the most intensive radiation in summer (Vähätalo et al. 2003). This small seasonal decrease in the photochemical reactivity is obviously below the accuracy of the method used, which explains the lack of seasonality in $\phi_{DIC,\lambda}$ and $\phi_{NH4,\lambda}$ in the Baltic Sea (see details in **III**).

The bacterial biomass responses to photoproduced labile substrates differed significantly between the studied seasons (**III**). As shown in Fig. 4C,

the ϕ_λs determined in July were highest in all sampling sites of **III**. The photostimulation of bacterial biomass is a biological process which is related e.g., to the seasonal changes in the bacterial community. For example, the probable occurrence of bacterial strains with a high affinity for photoproduced DOM generated the high ϕ_λs for photoproduction of labile substrates supporting bacterial biomass during summer. In **I**, similar temporal variation was seen in the bacterial production responses in the *in situ* -irradiation experiments. In addition to the composition of the bacterial assemblage, the changes in nutrient availability and low temperature either during the irradiations or the bacterial incubations may have influenced the temporal variation in the bacterial biomass (details in **I**).

4.5 SALINITY

This thesis studied the photochemical transformation of DOM in three salinity gradients: in the archipelago of Gulf of Finland (*Pj-A1* in Fig. 2; **I**), across the whole Baltic Sea (*NB-AS* in Fig. 2; **III**), and in the St. Lawrence River Estuary (0-31 in Fig. 3; **IV**).

In the small-scale salinity gradient (range of salinity 0 – 6) in the Gulf of Finland, the concentrations of DOM and its constituents were similar from the archipelago (*Lå*) to the open-sea (*A1*) but higher in the freshwater end of the salinity gradient (*Pj*; details in **I**). However, the effects of DOM phototransformation in bacterial production did not depend on the salinity (Fig. 4 in **I**).

The large-scale salinity gradient (range of salinity 1 – 8) in the Baltic Sea (**III**) was also a gradient for decreasing concentrations of DOC and $a_{CDOM,300}$ towards higher salinities (Table 2 in **III**). The photoproduction of DIC and the $\phi_{DIC,\lambda}$ followed the same trend (Fig. 4B). On the other hand, the concentration of DON and the amount of photoammonification were not related to the salinity. But after normalized the photoammonification with the absorbed photons, the $\phi_{NH4,\lambda}$ increased towards higher salinities (Fig. 4A; Fig. 4 in **III**). Unlike $\phi_{DIC,\lambda}$ and $\phi_{NH4,\lambda}$, the mean ϕ_λ for photoproduction of labile substrates supporting bacterial biomass over the seasons did not depend on the salinity (Fig. 4C). Evidently, the bacterial assemblages were similar enough over the studied ranges of salinity (0 – 6 and 1 – 8) in the Baltic Sea to give a similar bacterial response based on the labile photoproducts (**I**, **III**).

The samples collected along the salinity gradient of 0 – 31 in the St. Lawrence River Estuary represented a mixture of riverine and marine DOC (**IV**). The photoproduction of DIC and ϕ_{DIC} decreased towards higher salinities (Fig. 4B; Tables 2-3 in **IV** and Fig. 3 in **IV**) similarly to the salinity gradient in the Baltic Sea studying photoproduction of DIC in this thesis.

The results from this thesis support previous findings that the photoreactivity of DOC is higher in the low salinities (Bélanger et al. 2006,

White et al. 2010), where the photoreactivity of DON is the lowest (Stedmon et al. 2007, Morell & Corredor 2001). Further, this thesis and most of the previous studies indicate that terrigenous DOC is more photoreactive than marine DOC, but in terms of photoammonification, marine DON is more reactive than terrigenous DON.

4.6 PHOTOREACTION RATES

The apparent quantum yield spectrum (ϕ_λ) was applied in the Eq. 2 with the estimated solar irradiance spectrum (Q_λ) for each study area and season to calculate the rates for each photoreaction (details in **II**-**IV**). Although the solar irradiance increased towards the visible part of the spectrum, the ϕ_λs increased exponentially towards the UV range of the spectrum which was mainly responsible for the photoreactions. The rates for all photoreactions determined in this thesis peaked at a wavelength around 330 – 350 nm.

After integration the photoreaction rates over the spectrum in the Baltic Sea (**III**), the seasonal photoreaction rates over the water column were corrected with the mean seasonal temperatures of the surface water (details in **III**). Further, the seasonal rates were summed as annual rates (Fig. 5). The rates for photoammonification and photoproduction of DIC followed the salinity dependence of $\phi_{NH4,330}$ and $\phi_{DIC,330}$, respectively. Thus, in the freshwater site of Neva Bay, also the rates were highest for the photoproduction of DIC and lowest for the photoammonification (Fig. 5A and B). The summer rates were highest for all photoreactions due to the highest solar irradiance and the highest water temperature (see details in **III** for temperature correction of the modelled rates). Additionally, the highest ϕ_λs for the photostimulation of bacterial biomass in the summer resulted in the summer rates contributing 56 – 73% to the annual rates. The photoproduction rate of DIC exceeded several fold the other photoreaction rates studied (Fig. 5) indicating that DIC was the dominant product of DOM phototransformation.

In **II**, the natural sunlight induced photoproduction of labile substrates stimulated bacterial biomass by 164 μmol C m^{-2} d^{-1} and increased PON (labile N bound by hetero- and autotrophs) by 12 μmol N m^{-2} d^{-1} during a 12-d bioassay over the entire water column in the Baltic Sea in the summer. The very similar corresponding summer rates from the Gulf of Finland (**III**), where the irradiation with a sun simulator was followed by a 7-d bioassay, amounted to 130 μmol C m^{-2} d^{-1} as increase in the bacterial biomass and to 10 μmol N m^{-2} d^{-1} as increase in the NH_4^+ concentration. In the northern Baltic Sea in general, this magnitude of photostimulated bacterial production corresponds up to 4.5% of daily mean annual bacterial productivity (Sandberg et al. 2004) and provides a link of allochthonous DOM to the coastal food webs via bacterial grazing. The estimated magnitude of photoproduced N (NH_4^+ and labile N) can potentially support up to 3.6% of

the N demand of new primary production in the Gulf of Finland during summer (Vähätalo & Järvinen 2007).

In **III**, the annual photoreaction rates per m² (Fig. 5) were extrapolated to the annual rates across the entire Baltic Sea taking into account the salinity dependence of the photoreactions for photoammonification and photoproduction of DIC (details in **III**). Because the photostimulation of bacterial biomass was independent of salinity, the mean seasonal rates per m² of the study sites were extended over the entire area of the Baltic Sea. As a result, the photochemical reactions mineralized annually 0.038 – 0.049 Tg DON and 1.57 – 2.24 Tg DOC, and produced labile substrates, which supported 0.34 – 0.43 Tg C of bacterial biomass across the whole Baltic Sea (Table 6 in **III**).

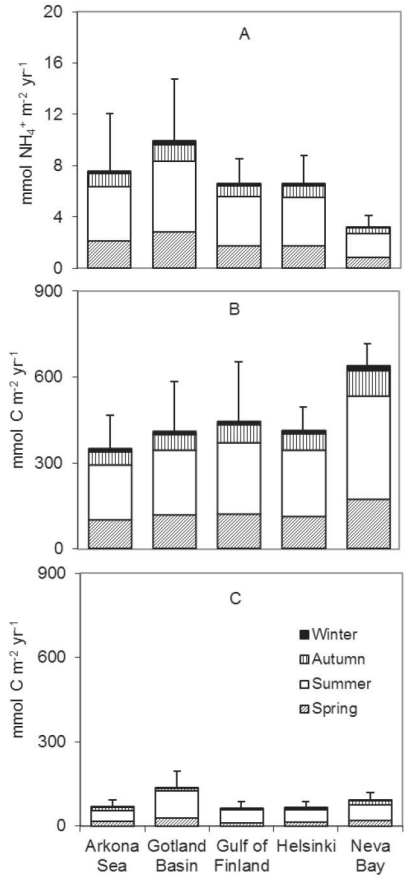

Figure 5 Sum of seasonal photoproduction rates of (a) NH_4^+, (b) DIC, and (c) labile substrates supporting bacterial biomass over the entire water column (Fig. 7 in **III**). Error bars describe the standard deviation of the methods (details in **III**).

In **IV**, the rates for photomineralization of terrigenous DOC were determined in a seawater matrix in order to approximate DIC photoproduction from riverine DOC along its transport from river mouth to offshore where nearly half of riverine CDOM was photobleached. Similar to the $\phi_{DIC,\lambda}$s, the annual rate of DIC photoproduction from riverine DOC was highest in the front of Mississippi River. On the other hand, the lowest annual photomineralization rate was for riverine DOC from Lena River (Fig. 4 in **IV**) despite of the high photoreactivity of terrigenous DOC ($\phi_{DIC,\lambda}$). The low annual intensity of solar irradiation in the Arctic region resulted in such a low photomineralization rate.

Further, the linear dependence between DIC photoproduction and the terrigenous CDOM photobleaching (Fig. 1 in **IV**) was used to estimate the annual DIC photoproduction from annual terrigenous CDOM flux of each river resulting in a sum of 12.5 ± 2.1 Tg C y^{-1} (Table 3). This estimate corresponds 18 ± 4% to the annual terrigenous DOC flux in the studied rivers (Table 4 in **IV**). Assuming that the same proportion of total global riverine terrigenous DOC flux (246 Tg C yr^{-1}; Cai, 2011) will be photomineralized to DIC as in the studied rivers (**IV**), the global photomineralization of terrigenous DOC corresponds to 44.5 ± 10.6 Tg C yr^{-1} in the global coastal ocean. This estimate for the global coastal ocean is more than a corresponding global estimate of DIC photoproduction from terrigenous DOC in lakes and reservoirs (13 to 35 Tg C yr^{-1}; Koehler et al. 2014), indicating that solar radiation mineralizes terrigenous DOC mainly in the coastal ocean rather than in the inland waters. However, the areal rates of DIC photoproduction are larger in the freshwaters than in the coastal waters (details in **IV**). This indicates that in the inland waters, the phototransformation of terrigenous DOC is likely mainly limited by short residence times compared to the ones in the coastal ocean leading to an extensive export of photoreactive DOC (or CDOM) to the coastal ocean (Fig. 6 in **IV**).

Table 3 *Annual photoproduction of DIC from riverine CDOM flux, and the area and distance required for photomineralization of riverine DOC flux (mean ± SD; details in **IV**).*

River	Photoproduction of DIC Tg C yr^{-1}	Photomineralization area for DOC 10^3 km^2	Photomineralization distance for DOC km
Amazon	6.98 ± 1.08	4 286 ± 1 096	1 652 ± 422
Congo	3.04 ± 0.49	1 899 ± 318	1 099 ± 184
Danube	0.08 ± 0.02	91 ± 38	240 ± 100
Ganges-Brahmaputra	0.13 ± 0.06	194 ± 115	351 ± 209
Lena	1.36 ± 0.24	2 186 ± 533	1 180 ± 288
Mekong	0.13 ± 0.04	141 ± 46	299 ± 99
Mississippi	0.24 ± 0.05	130 ± 26	287 ± 58
Paraná	0.23 ± 0.05	270 ± 89	415 ± 136
St. Lawrence	0.07 ± 0.01	76 ± 19	221 ± 54
Yangtze	0.23 ± 0.07	352 ± 209	474 ± 282
Total	12.48 ± 2.10	9 624 ± 2 489	Median 383 ± 160

4.6.1 COMPARISON BETWEEN MEASURED (*IN SITU*) AND MODELLED RATES

For validation of the modelled photomineralization of DOC to DIC, the modelled and measured (*in situ*) rates were compared in the Lake Pääjärvi (**III**). The measured rates for photomineralization of DOC declined steeply with the water depth (Fig. 2 in **III**), as the photoreactive solar irradiation attenuated in the top 30 cm of the mesohumic lake water. After integrating over the whole water column, the measured rates for photomineralization of DOC were 1079 and 1280 μmol C m^{-2} d^{-1} in July and August, respectively (Table 1 in **III**) corresponding to <12% of the community respiration (by algae, bacteria, HNF, ciliates, and metazooplankton) in that mesohumic lake in summer (Kankaala et al. 1996). The rates in the mesohumic lake Pääjärvi were supposedly higher than the corresponding rates modelled in the Baltic Sea (Fig. 6E in **III**).

When the measured rates for photomineralization of DOC were compared to the modelled rates determined for the Lake Pääjärvi samples, the former were higher. However, the lake water temperature during the *in situ* experiments in July and August (17 – 19 °C) was higher than the temperature set for the laboratory irradiation experiments (5 °C; Table 1 in **III**). The temperature dependence of the photomineralization of DOC was assessed based on the measured and modelled rates by determining the activation energy, E_a (J mol^{-1}), of the Arrhenius equation (see details in **III**). When used the mean E_a (20.7 kJ mol^{-1}) determined for the photomineralization of DOC in the two irradiation experiments in the Lake Pääjärvi and accounted for the temperature difference, the difference between the modeled and measured rates was ± 5% (**III**). This indicates that the optical model (Eq. 2) used in this thesis described the photoreaction rates quite well, at least for the photoproduction of DIC.

In this thesis, the temperature dependence of photochemical reactions was determined according to the comparison of measured and modelled rates for photoproduction of DIC (**III**). Thus, the temperature dependence relies on only two temperatures and describes only one photoreaction, even though the estimated E_a was used for correcting also the rates of photoammonification and the photoproduction of labile DOM supporting bacterial biomass in **III**, as this information was the best available. However, when it is a question of phototransformation of DOM, the amount of irradiation is a far more important factor affecting the magnitude of photoreaction rates than is the temperature (see e.g., **III** and **IV**).

4.7 ENVIRONMENTAL RELEVANCE OF DOM PHOTOCHEMISTRY

The photochemical transformation of non-labile DOM to labile substrates supporting heterotrophic bacterial biomass forms a link of terrestrial carbon

to higher trophic levels via a microbial loop (**I**, **II**, **III**). To illustrate the significance of the magnitude of bacterial biomass grown on the expense of photoproduced labile substrates, it has been compared to the other annual C rates in the Baltic Sea (Table 6 in **III**). Across the entire Baltic Sea, the magnitude of photostimulated bacterial carbon biomass (0.34 – 0.43 Tg C yr^{-1}; **III**) corresponded e.g., to 3 – 5% of total bacterial production, 0.7 – 1.1% of phytoplankton production, or 7 – 24% of mesozooplankton production, or exceeded the fish catch in the Baltic Sea three- to six fold (Table 6 in **III**).

The magnitude of photoammonification in the Baltic Sea (0.038 – 0.049 Tg N yr^{-1}; **III**) corresponded e.g., to 13 – 23% of the atmospheric deposition of inorganic N, 9 – 18% of the riverine load of DON, or 20 – 56% of N_2 fixation by cyanobacteria in the Baltic Sea (Table 6 in **III**). Thus, the photoammonification may constitute an important source of inorganic N for bacterio- and phytoplankton in the surface waters during an event of N-depletion (Vähätalo & Järvinen 2007). However, as the growth of heterotrophic bacteria is mainly C limited for example in the northern Baltic Sea during the nutrient minimum (e.g., **I**), planktonic algae rather than bacteria will incorporate the photoproduced labile N, potentially increasing the magnitude and duration of algal blooms (Thingstad et al. 2008). On the other hand, **II** concluded that simultaneous photoproduction of labile C and N particularly supported bacteria over planktonic algae, and that N bound in bacteria may subsequently be transferred to algae by mixotrophy or as N released in grazing of bacteria (i.e., sloppy feeding).

The magnitude of the direct photomineralization of DOC to DIC across the Baltic Sea (1.57 – 2.24 Tg C yr^{-1}; **III**) corresponded to 32 – 106% of the riverine load of total organic carbon (TOC) in the Baltic Sea (Table 6 in **III**). The indirect photomineralization of DOC including the photostimulation of bacterial biomass as well as the bacterial respiration calculated with a bacterial growth efficiency (BGE) of 0.20 – 0.25 (details in **III**) contributed 72 – 76% to the direct photomineralization of DOC. When summing the direct and the indirect photomineralization of DOC, the resulting amount of 2.71 – 3.94 Tg C yr^{-1} equals the annual riverine input of terrestrial TOC to the Baltic Sea (2.11 – 4.90 Tg C yr^{-1}; Table 6 in **III**). However, only the photoreactive proportion of annual input of terrestrial TOC can be mineralized photochemically, and assuming that proportion to be half of the total input, the total photochemical mineralization of DOC in the Baltic Sea (2.71 – 3.94 Tg C yr^{-1}) exceeds the annual riverine input of photoreactive DOM (< 2.45 Tg C yr^{-1}) to the Baltic Sea. This indicates that photochemical reactions transform also autochthonous photoreactive DOM which is produced in the coastal waters.

Also in the global coastal ocean, the photochemical transformation of terrigenous DOM may equal the riverine inputs (Miller et al. 2002, Wang et al. 2009). **IV** suggested a global estimate (44.5 ± 10.6 Tg C yr^{-1}) for annual direct photomineralization of riverine non-labile DOC to DIC. When also the indirect photomineralization of riverine non-labile DOC by bacteria

(Kasurinen et al. unpublished) is taken into account, the total annual photostimulated mineralization of riverine DOC amounted to 82.5 ± 26.5 Tg C yr^{-1}. Thus, the total photomineralization of riverine DOC corresponded to 23 – 44% of the annual flux of photoreactive riverine DOC (246 Tg C yr^{-1}; Cai 2011) in the global coastal ocean.

The surface areas of coastal ocean required for the direct photolytic mineralization of photoreactive riverine DOC for each river (detailed calculations in **IV**) are represented in Table 3 and illustrated on the map of Fig. 5 in **IV**. The area was largest for the Amazon River and smallest for the St. Lawrence River as was the distance where the flux of riverine CDOM extends in the coastal ocean (Table 3; details in **IV**). Although this approach harshly simplifies the dispersion of riverine DOC in the coastal ocean, it demonstrates how the photomineralization of riverine DOC takes mainly place within a few hundred kilometres (median of 383 ± 160 km) from river mouths for most rivers studied excluding the largest discharges (Amazon and Congo Rivers) and the Arctic river, Lena (Table 3). This agrees with the earlier findings that the open ocean do not contain traces of terrigenous CDOM (Nelson & Siegel 2013), thus, the photobleaching in the coastal waters is the final sink for terrigenous photoreactive CDOM.

5 CONCLUSIONS

In the boreal lake examined, the photoreactive solar radiation attenuated steeply with the water depth and thus, the photomineralization of DOC was declined rapidly into the top 30 cm of the lake water column. The DIC photoproduction rate corresponded to about a tenth of the community respiration in summer in that mesohumic lake.

In the Baltic Sea, where the DOM pool is mostly biologically non-labile, the heterotrophic bacteria are limited by bioavailable C and inorganic nutrients in the surface water layer. Thus, the photochemical transformation of DOM may stimulate the bacterial growth by providing labile organic and inorganic substrates to the surface water, which can stimulate also heterotrophic nanoflagellates and ciliates via grazing. Simultaneously, DOM photochemistry may support the production of autotrophic algae by providing bioavailable nitrogen in the surface water during the period of thermal stratification and the nutrient minimum in summer. The magnitude of the direct photochemical mineralization of DOC to DIC was greater than the magnitudes of the other studied photoreactions in this thesis. In the Baltic Sea, the significance of DOM photochemistry can clearly be highlighted as, for example, the photochemical mineralization of DOM exceeds the annual riverine input of photoreactive DOM to the Baltic Sea.

Globally, solar radiation mineralizes terrigenous DOC mainly in the coastal ocean rather than in the inland waters. Short residence times potentially limit the phototransformation of terrigenous DOC in the inland waters, which leads to an extensive export of photoreactive terrigenous DOC to the coastal ocean. As the open ocean contains no traces of terrigenous CDOM, the photobleaching in the coastal waters is the final sink for terrigenous CDOM and thus, also for photoreactive terrigenous DOC.

In this thesis, the focus was in the quantification of the photochemical reaction rates and the environmental relevance of the photochemical transformation processes. The composition of DOM was not investigated broadly in this thesis, even though the structure and composition of DOM molecules affect the photochemical reactivity and thus, the DOM phototransformation rates. As a future work, the relationship between the composition and the decomposition of DOM could be examined more closely. Similarly, as the temperature dependence of the photoreactions was determined only for the photoproduction of DIC and with only two temperatures in this thesis, a future work could assess more precise values for the activation energy (E_a) of different photoreactions transforming DOM.

ACKNOWLEDGEMENTS

After ten years of work – with almost a 5-year pause when working at UN in Kenya and raising two wonderful sons at home – you can finally hold this book on your hands. Life is a mystery.

I greatly acknowledge my thesis' pre-examiners prof. Roger Jones and prof. David Kieber for their valuable comments. I thank the Academy of Finland for funding most of the time I worked with the thesis, and Maa- ja vesitekniikan tuki ry and University of Helsinki for the financial support at the final stage. My graduate school EnSTe enabled me to meet fellow PhD students from other Finnish universities, provided interesting and useful courses and also financial support e.g., for travelling to conferences, and I am thankful for the possibility to be a member.

Along these years, there are so many people to be grateful for. I feel privileged to meet all those nice and helpful people during my work. The greatest thanks go to my one and only supervisor Anssi Vähätalo without whom I would have never even chosen this topic, felt moments of scientific enthusiasm around the topic of aquatic photochemistry, or in the end, reached this goal. Thanks for your patience. The first paper of my thesis is based on the data collected for my master's thesis supervised by Risto Lignell and I thank him for introducing the interesting world of DOM to me. Laura Hoikkala is thanked for sharing the work load with me and for being a great friend from the day one. I also thank my other co-authors Pasi Ylöstalo, Yves Gélinas and Ville Kasurinen for their contributions to the papers in this thesis. I cannot forget the assistance of undergraduate, ERASMUS, and laboratorian students involved in my work during these years; it has been a pleasure and lots of fun to work with you.

Several institutes and departments have facilitated this work and I am happy to be able to work in many places with different people around me. The section of Aquatic Sciences in Viikki is my scientific home and the place where it all started. I am sure I will always miss my fellow PhD students and the other great colleagues, but also the community spirit for example in legendary "pikkujoulut" at Café Limnos. Our DOM-group and all AKVA-people in Viikki, thanks for your support and sharing your scientific and non-scientific life with me. The experimental work for two papers of this thesis was conducted in Tvärminne Zoological Research Station and I thank especially the laboratory staff for their assistance. The former Finnish Institute of Marine Research is thanked for providing the facilities for epifluorescence microscoping. Lammi Biological Station hosted part of the experiments of this thesis and I like to thank all the staff for their support and friendship, and for making me feel like home at the station. At the final stage, the department of Biological and Environmental Science, University of Jyväskylä facilitated my work, which I am truly grateful. The warm and

welcoming working community at “Ymppi” delighted me, while I was finalizing the thesis and the last manuscript. Thank you all for having me as a part of the team. Special thanks go to my room mates both in Viikki and Jyväskylä; without your support and nice words the work would have been much harder.

Fortunately the non-scientific friends of mine in addition to my family have given me other thoughts besides the work, and I am grateful for their company and time. My mom has been priceless for taking care of the boys during the last months of this work. Finally, I thank my husband Kari for unlimited support, love and patience during the years together. Lauri and Eino, my dearest boys, you show me every day what is important in life. Thanks for being.

REFERENCES

Amon R. M. W. & Benner R. Rapid cycling of high-molecular-weight dissolved organic matter in the ocean. *Nature* 369: 549-552, 1994.

Amon R. M. W. & Benner R. Bacterial utilization of different size classes of dissolved organic matter. *Limnol. Oceanogr.* 41: 41–51, 1996.

Andrews S. S., Caron S., Zafiriou O. C. & Zafirioul O. C. Photochemical Oxygen Consumption in Marine Waters: A Major Sink for Colored Dissolved Organic Matter? *Limnol. Oceanogr.* 45: 267–277, 2000.

Arvola L., Kankaala P., Tulonen T. & Ojala A. Effects of phosphorus and allochthonous humic matter enrichment on the metabolic processes and community structure of plankton in a boreal lake (Lake Pääjärvi). *Can. J. Fish. Aquat. Sci.* 53: 1646–1662, 1996.

Azam F., Fenchel T., Field J. G., Meyer-Reil L.-A. & Thingstad F. The ecological role of water-column microbes in the sea. *Mar. Ecol. Prog. Ser.* 10: 257–263, 1983.

Bélanger S., Xie H. X., Krotkov N., Larouche P., Vincent W. F. & Babin M. Photomineralization of terrigenous dissolved organic matter in Arctic coastal waters from 1979 to 2003: Interannual variability and implications of climate change. *Global Biogeochem. Cycles*, 20(4), GB4005, 2006.

Bertilsson S. & Tranvik L. J. Photochemical transformation of dissolved organic matter in lakes. *Limnol. Oceanogr.* 45(4): 753-762, 2000.

Bushaw K., Zepp R., Tarr M., Schulz-Jander D., Bourbonniere R., Hodson R., Miller W., Bronk D. & Moran M. A. Photochemical release of biologically available nitrogen from aquatic dissolved organic matter. *Nature* 381: 404–407, 1996.

Cai W.-J. Estuarine and Coastal Ocean Carbon Paradox: CO_2 Sinks or Sites of Terrestrial Carbon Incineration? *Annual Review of Marine Science* 3: 123–145, 2011.

Carlson C. A. & Hansell D. A. DOM Sources, Sinks, Reactivity, and Budgets. *In* Biogeochemistry of Marine Dissolved Organic Matter, 2nd Edition, edited by Hansell, D. A. and Carlson, C. A., Chapter 3, pp. 65-126, Elsevier, 2015.

Cauwet, G. DOM in the Coastal Zone. *In* Biogeochemistry of Marine Dissolved Organic Matter, edited by Hansell, D. A. and Carlson, C. A., Chapter 12, pp. 579–609, Elsevier, 2002.

Cory R. M., Ward C. P., Crump B. C. & Kling G. W. Sunlight controls water column processing of carbon in arctic fresh waters. *Science* 345: 925–928, 2014.

Daniel C., Granéli W., Kritzberg E. S. & Anesio A. M Stimulation of metazooplankton by photochemically modified dissolved organic matter. *Limnol. Oceanogr.* 51: 101–108, 2006.

De Lange H. J., Morris D. P. & Williamson C. E. Solar ultraviolet photodegradation of DOC may stimulate freshwater food webs. *J. Plankton Res.* 25: 111–117, 2003.

Fenchel T. Marine plankton food chain. *Ann. Rev. Ecol. Syst.* 19: 19–38., 1988.

Granéli W., Lindell M. & Tranvik L. Photo-oxidative production of dissolved organic carbon in lakes of different humic content. Limnol. Oceanogr. 41(4): 698-706, 1996.

Groeneveld M., Tranvik, L. J. & Koehler B. Photochemical mineralization in a humic boreal lake: temporal variability and contribution to carbon dioxide production. *Biogeosciences Discuss*., 12, 17125-17152, 2015.

Hansell D. A., Carlson C. A., Repeta D. J. & Schlitzer R. Dissolved organic matter in the ocean: a controversy stimulates new insights. *Oceanography* 22: 202-211, 2009.

Hansell, D. A. Recalcitrant dissolved organic carbon fractions. *In* Ann. Rev. Mar. Sci. Vol 5, edited by Carlson C. C & Giovannoni S. J., pp. 421–445, 2013.

He W., Chen M., Schlautman M. A. & Hur J. Dynamic exchanges between DOM and POM pools in coastal and inland aquatic ecosystems: A review. *Science of the Total Environment* 551-552: 415-428, 2016.

Hedges J. I. Global biochemical cycles: Progress and problems. *Mar. Chem.* 39: 67-93, 1992.

Hedges J. I. Why Dissolved Organics Matter. *In* Biogeochemistry of Marine Dissolved Organic Matter, edited by Hansell D. A. & Carlson C. A., Chapter 1, pp. 1-34, Elsevier, 2002.

Hoikkala L., Kortelainen P., Soinne H. & Kuosa H. Dissolved organic matter in the Baltic Sea. *Journal of Marine Systems*, 142, 47-61, 2015.

Jaffé R., Ding Y., Niggemann J., Vähätalo A. V., Stubbins A., Spencer R. G., Campbell J. & Dittmar T. Global charcoal mobilization from soils via dissolution and riverine transport to the oceans. *Science* 340: 345–347, 2013.

Johannessen S. C. & Miller W. L. Quantum yield for the photochemical production of dissolved inorganic carbon in seawater. *Mar. Chem*., 76(4), 271–283, 2001.

Johannessen S. C., Peña M. A. & Quenneville M. L. Photochemical production of carbon dioxide during a coastal phytoplankton bloom. *Estuarine, Coastal and Shelf Science* 73, 236-242, 2007.

Jumars P., Penry D., Baross J., Perry M. & Frost B. Closing the microbial loop: Dissolved carbon pathway to heterotrophic bacteria from incomplete ingestion, digestion and absorption in animals. *Deep-Sea Res.* 36: 483–495, 1989.

Kieber D. J., McDaniel J. & Mopper K. Photochemical source of biological substrates in sea water: implications for carbon cycling. *Nature* 341: 637-639, 1989.

Kieber R. J., Zhou X. & Mopper K. Formation of carbonyl compounds from UV-induced photodegradation of humic substances in natural waters: Fate of riverine carbon in the sea. *Limnol. Oceanogr.* 35(7): 1503-1515, 1990.

Koehler B., Landelius T., Weyhenmeyer G. A., Machida N. & Tranvik L. J. Sunlight-induced carbon dioxide emissions from inland waters. *Global Biogeochemical Cycles*, 28, 696–711, 2014.

Kuparinen J. & Heinänen A. Inorganic Nutrient and Carbon Controlled Bacterioplankton Growth in the Baltic Sea. *Estuarine, Coastal and Shelf Science* 37: 271–285, 1993.

Lalonde K., Vähätalo A. V. & Gélinas Y. Revisiting the disappearance of terrestrial dissolved organic matter in the ocean: a $\delta^{13}C$ study. *Biogeosciences* 11: 3707–3719, 2014.

Lampert W. Release of dissolved organic carbon by grazing zooplankton. *Limnol. Oceanogr.* 23: 831–834, 1978.

Leppäranta M. & Myrberg K. Physical Oceanography of the Baltic Sea. 378 pp., Springer, Berlin, 2009.

Lignell R., Kaitala S. & Kuosa H.. Factors controlling phyto- and bacterioplankton in late spring on a salinity gradient in the northern Baltic. *Marine Ecology Progress Series* 86: 273–281, 1992.

Lignell R., Hoikkala L. & Lahtinen T. Effects of inorganic nutrients, glucose and solar radiation treatments on bacterial growth and exploitation of dissolved organic carbon and nitrogen in the northern Baltic Sea. *Aquatic Microbial Ecology* 51: 209–221, 2008.

Lindell M. J., Granéli W. & Tranvik L. J. Enhanced bacterial growth in response to photochetiical transformation of dissolved organic matter. *Limnol. Oceanogr.* 40(1): 195-199, 1995.

Medeiros P. M., Seidel M., Ward N. D., Carpenter E. J., Gomes H. R., Niggemann J., Krusche A. V., Richey J. E., Yager P. L. & Dittmar T. Fate of the Amazon River dissolved organic matter in the tropical Atlantic Ocean. *Global Biogeochemical Cycles* 29(5): 677-690, 2015.

Miller W. L. & Zepp R. G. Photochemical production of dissolved inorganic carbon from terrestrial organic matter: Significance to the oceanic organic carbon cycle. *Geophysical Research Letters* 22(4): 417-420, 1995.

Miller W. L. & Moran M. A. Interaction of photochemical and microbial processes in the degradation of refractory dissolved organic matter from a coastal marine environment. *Limnol. Oceanogr.* 42: 1317-1324, 1997.

Miller W. L., Moran M. A., Sheldon W. M., Zepp R. G. & Opsahl S. Determination of apparent quantum yield spectra for the formation of biologically labile photoproducts, *Limnol. Oceanogr.* 47(2): 343–352, 2002.

Milliman J. D. & Farnsworth K. L. River Discharge to the Coastal Ocean: A Global Synthesis. Vol. 24, pp. 384, Cambridge University Press, Cambridge, 2011.

Molot L. A. & Dillon P. J. Photolytic regulation of dissolved organic carbon in northern lakes. *Global Biogeochemical Cycles 11*: 357-365, 1997.

Mopper K., Zhou X., Kieber R. J., Kieber D. J., Sikorski R. J. & Jones R. D. Photochemical degradation of dissolved organic carbon and its impact on the oceanic carbon cycle. Nature 353: 60-62, 1991.

Mopper K., Kieber D. J. & Stubbins A. Marine Photochemistry of Organic Matter: Processes and Impacts. *In* Biogeochemistry of Marine Dissolved Organic Matter, 2nd Edition, edited by Hansell D. A. & Carlson C. A., Chapter 8, pp. 389-450, Elsevier, 2015.

Moran M. A. & Zepp R. G. Role of photoreactions in the formation of biologically labile compounds from dissolved organic matter *Limnol. Oceanogr.* 42(6): 1307–1316, 1997.

Morell J. M. & Corredor J. E. Photomineralization of fluorescent dissolved organic matter in the Orinoco River plume: Estimation of ammonium release. *J. Geophys. Res.* 106(C8): 16,807–16,813, 2001.

Nagata T. Production mechanisms of dissolved organic matter. *In* Microbial ecology of the oceans, edited by Kirchman D. L., pp. 121–152. Wiley-Liss, New York, 2000.

Nelson N. B. & Siegel D. A. The global distribution and dynamics of chromophoric dissolved organic matter. *Annual Review of Marine Science* 5: 447–76, 2013.

Powers L. & Miller W. Photochemical production of CO and CO2 in the Northern Gulf of Mexico: Estimates and challenges for quantifying the impact of photochemistry on carbon cycles. *Marine Chemistry* 171, 21-35, 2015.

Reader H. & Miller W. Variability of carbon monoxide and carbon dioxide apparent quantum yield spectra in three coastal estuaries of the South Atlantic Bight. *Biogeosciences* 9, 4279-4294, 2012.

Salonen K. Rapid and precise determination of total inorganic carbon and some gases in aqueous solutions. *Water Res.* 15(4): 403–406, 1981.

Sandberg J., Andersson A., Johansson S. & Wikner J. Pelagic food web structure and carbon budget in the northern Baltic Sea: Potential importance of terrigenous carbon. *Mar. Ecol. Prog. Ser.* 268: 13–29, 2004.

Siegenthaler U. & Sarmiento J.L. Atmospheric carbon dioxide and the ocean. *Nature* 365: 119–125, 1993.

Søndergaard M. & Middelboe M. A cross-system analysis of labile dissolved organic carbon. *Mar. Ecol. Prog. Ser.* 118: 283-294, 1995.

Stedmon C. A., Markager S., Tranvik L., Kronberg L., Slätis T. & Martinsen W. Photochemical production of ammonium and transformation of dissolved organic matter in the Baltic Sea. *Marine Chemistry* 104(3-4): 227-240, 2007.

Tarr M. A., Wang W., Bianchi T. S. & Engelhaupt E. Mechanisms of ammonia and amino acid photoproduction from aquatic humic and colloidal matter. *Water Res.* 35: 3688–3696, 2001.

Thingstad T. F. & Lignell R. Theoretical models for the control of bacterial growth rate, abundance, diversity and carbon demand. *Aquatic Microbial Ecology* 13: 19–27, 1997.

Thingstad T. F., Bellerby R. G. J., Bratbak G., Borsheim K. Y., Egge J. K., Heldal M., Larsen A., Neill C., Nejstgaard J., Norland S., Sandaa R.A., Skjoldal E.F., Tanaka T., Thyrhaug R. & Topper B. Counterintuitive carbon-to-nutrient coupling in an Arctic pelagic ecosystem. *Nature* 455(7211): 387–390, 2008.

Vähätalo A. V., Salkinoja-salonen M., Taalas P., & Salonen K. Spectrum of the quantum yield for photochemical mineralization of dissolved organic carbon in a humic lake. *Limnol. Oceanogr.*, 45, 664–676, 2000.

Vähätalo A., Salonen K., Münster U., Järvinen M. & Wetzel R.G. Photochemical transformation of allochtonous organic matter provides bioavailable nutrients in a humic lake. *Archiv für Hydrobiologie* 156: 287–314, 2003.

Vähätalo A. V. & Wetzel R. G. Photochemical and microbial decomposition of chromophoric dissolved organic matter during long (months–years) exposures. *Mar. Chem.* 89(1–4): 313–326, 2004.

Vähätalo A. V. & Zepp R. G. Photochemical mineralization of dissolved organic nitrogen to ammonium in the Baltic Sea. *Environ. Sci. Technol.*, 39(18), 6985–6992, 2005.

Vähätalo A. V. & Järvinen M. Photochemically produced bio-available nitrogen from biologically recalcitrant dissolved organic matter stimulates production of a nitrogen-limited microbial food web in the Baltic Sea. *Limnol. Oceanogr.*, 52(1), 132–143, 2007.

Vähätalo A. V. Light, Photolytic Reactivity and Chemical Products. *In* Encyclopedia of Inland Waters, edited by Likens G. E., vol. 2, pp. 761-773, Elsevier, Oxford, 2009.

Wagner S., Riedel T., Niggemann J., Vähätalo A. V., Dittmar T. & Jaffé R. Linking the Molecular Signature of Heteroatomic Dissolved Organic Matter to Watershed Characteristics in World Rivers. *Environ. Sci. Technol.* 49(23): 13798-13806, 2015.

Wang W., Johnson C. G., Takeda K. & Zafiriou O. C. Measuring the photochemical production of carbo dioxide from marine dissolved organic matter by pool isotope exchange. *Environ. Sci. Technol.* 43: 8604-8609, 2009.

Wetzel R. G., Hatcher P. G. & Bianchi T. S. Natural photolysis by ultraviolet irradiance of recalcitrant dissolved organic matter to simple substrates for rapid bacterial metabolism. *Limnol. Oceanogr.* 40(8): 1369-1380, 1995.

Wetzel R. G. Limnology. Lake and river ecosystems. 3rd edition, Academic Press, New York. Pp. 1006, 2001.

White E. M., Kieber D. J., Sherrard J., Miller W. L. & Mopper K. Carbon dioxide and carbon monoxide photoproduction quantum yields in the Delaware Estuary, *Marine Chemistry*, 118, 11–21, 2010.

Zubkov M. V. & Tarran G. A. High bacteriovory by the smallest phytoplankton in the North Atlantic Ocean. *Nature* 455: 224–227, 2008.

Xiao Y.-H., Sara-Aho T., Hartikainen H. & Vähätalo A. V. Contribution of ferric iron to light absorption by chromophoric dissolved organic matter, *Limnol. Oceanogr.* 58: 653–662, 2013.

Recent Publications in this Series

1/2016 Hanna Help-Rinta-Rahko
The Interaction Of Auxin and Cytokinin Signalling Regulates Primary Root Procambial Patterning, Xylem Cell Fate and Differentiation in *Arabidopsis thaliana*
2/2016 Abbot O. Oghenekaro
Molecular Analysis of the Interaction between White Rot Pathogen *(Rigidoporus microporus)* and Rubber Tree *(Hevea brasiliensis)*
3/2016 Stiina Rasimus-Sahari
Effects of Microbial Mitochondriotoxins from Food and Indoor Air on Mammalian Cells
4/2016 Hany S.M. EL Sayed Bashandy
Flavonoid Metabolomics in *Gerbera hybrida* and Elucidation of Complexity in the Flavonoid Biosynthetic Pathway
5/2016 Erja Koivunen
Home-Grown Grain Legumes in Poultry Diets
6/2016 Paul Mathijssen
Holocene Carbon Dynamics and Atmospheric Radiative Forcing of Different Types of Peatlands in Finland
7/2016 Seyed Abdollah Mousavi
Revised Taxonomy of the Family *Rhizobiaceae*, and Phylogeny of Mesorhizobia Nodulating *Glycyrrhiza spp*.
8/2016 Sedeer El-Showk
Auxin and Cytokinin Interactions Regulate Primary Vascular Patterning During Root Development in *Arabidopsis thaliana*
9/2016 Satu Olkkola
Antimicrobial Resistance and Its Mechanisms among *Campylobacter coli* and *Campylobacter upsaliensis* with a Special Focus on Streptomycin
10/2016 Windi Indra Muziasari
Impact of Fish Farming on Antibiotic Resistome and Mobile Elements in Baltic Sea Sediment
11/2016 Kari Kylä-Nikkilä
Genetic Engineering of Lactic Acid Bacteria to Produce Optically Pure Lactic Acid and to Develop a Novel Cell Immobilization Method Suitable for Industrial Fermentations
12/2016 Jane Etegeneng Besong epse Ndika
Molecular Insights into a Putative Potyvirus RNA Encapsidation Pathway and Potyvirus Particles as Enzyme Nano-Carriers
13/2016 Lijuan Yan
Bacterial Community Dynamics and Perennial Crop Growth in Motor Oil-Contaminated Soil in a Boreal Climate
14/2016 Pia Rasinkangas
New Insights into the Biogenesis of *Lactobacillus rhamnosus GG* Pili and the *in vivo* Effects of Pili
15/2016 Johanna Rytioja
Enzymatic Plant Cell Wall Degradation by the White Rot Fungus *Dichomitus squalens*
16/2016 Elli Koskela
Genetic and Environmental Control of Flowering in Wild and Cultivated Strawberries
17/2016 Riikka Kylväjä
Staphylococcus aureus and *Lactobacillus crispatus*: Adhesive Characteristics of Two Gram-Positive Bacterial Species

Helsinki 2016 ISSN 2342-5423 ISBN 978-951-51-2357-2